TECHNICAL NOTES

NATIONAL ADVISORY COMMITTEE FOR AERONAUTICS

No. 918

THE STABILITY OF ISOTROPIC OR ORTHOTROPIC CYLINDERS OR FLAT OR CURVED PANELS, BETWEEN AND ACROSS STIFFENERS, WITH ANY EDGE CONDITIONS BETWEEN HINGED AND FIXED, UNDER ANY COMBINATION OF COMPRESSION AND SHEAR

By L. H. Donnell
Chance Vought Aircraft

Washington
December 1943

NOTATION

Symbol	Paragraph
a, b	26
a, b (subscripts)	87
a', b'	42, 48
$a_1 .. a_i .. a_6$ $b_1 .. b_i .. b_5$ $c_1 .. c_i .. c_8$ $d_1 .. d_i .. d_6$	30, 114, 115
A, B, C, D	17 – 21
A_a', A_b'	45, 48
$A_1 .. A_i .. A_6$ $B_1 .. B_i .. B_5$ $C_1 .. C_i .. C_8$	25
Case A	30
Case B	40
Case A', B'	41
	26
A', B', C', D' $D+, D-$	Tables I, III
d_a, d_b	93
d_o	Table I
$D_1 .. D_i .. D_8$	24
e	16
E, E_L, E_R	15, 16
E_a, E_a', E_b, E_b'	43, 44, 48, 51
ϵ	16
$f_\alpha, f_\beta, f_{\alpha\beta}$	88
F_a, F_b, F_s	26
g	16
G_{LT}, G_{RT}	15
$G_a'J_a', G_b'J_b'$	46, 48
$G_a''J_a'', G_b''J_b''$	54, 56
h_a, h_b	45, 48
H	16
K_1, K_2	27, 29
K_a, K_b	54, 56
m, n	Fig. 3a, b
"Critical" m, n	29
n'	108
$m_\alpha, m_\beta, m_{\alpha\beta}$	88
M, N, P, Q	24
r	Fig. 3a, b
s_a, s_b, s_s	114

Symbol	Paragraph	Symbol	Paragraph
S	30	γ	30
S_a, S_b, S_s	26	$\Delta_1, \Delta_2, \Delta_a, \Delta_b$	53, 56
S_a', S_b'	50	ϵ	16
$S_{mat\ strength}$, $S_{theor\ stab}$	27	$\epsilon_a, \epsilon_b, \epsilon_{ab}$; $\epsilon_\alpha, \epsilon_\beta, \epsilon_{\alpha\beta}$	88, 93
$S+, S-$	Table I	θ	23
t	17	$\kappa_a, \kappa_b, \kappa_{ab}$; $\kappa_\alpha, \kappa_\beta, \kappa_{\alpha\beta}$	88, 95
$t_1, t_2 .. t_i, t_j$	17	λ	30
t'	29	μ, μ_{TL}, μ_{RL}	15, 16
T, V, T', V'	89, 97, 98, 102	ρ_a, ρ_b	45, 48
$u_a, u_b, u_\alpha, u_\beta$	87		
U_a, U_b	112		
w	87		
w_a, w_b	45, 48		
W	104		
$x_a, x_b, x_\alpha, x_\beta$	87		
X, Y	24		
z	Table I		
α, β	30		
α, β (subscripts or directions)	87		

NATIONAL ADVISORY COMMITTEE FOR AERONAUTICS

TECHNICAL NOTE NO. 918

THE STABILITY OF ISOTROPIC OR ORTHOTROPIC CYLINDERS OR FLAT OR CURVED PANELS, BETWEEN AND ACROSS STIFFENERS, WITH ANY EDGE CONDITIONS BETWEEN HINGED AND FIXED, UNDER ANY COMBINATION OF COMPRESSION AND SHEAR

By L. H. Donnell*

INTRODUCTION

1. Most "theories" are derived for rather simple idealized cases, and when it comes to applying them to practical problems many important factors must be entirely neglected, or their effects guessed at. In this report a deliberate effort has been made to include all the factors which are commonly present, and which have an important effect on the final result, with as high a degree of accuracy as present knowledge of the subject permits.

2. A theory covering such a wide range cannot be expected to be reduced to simple formulas or charts. It has been, however, put in such form that anyone familiar with calculating and plotting can study a considerable range of practical applications with from a few hours to a few days of work. That is, the work involved is somewhat similar to that required for solving a statically indeterminate structure. Much simpler methods, of course, can be developed for more limited applications (see, for example, reference 1 or 2) and these should be used where they are applicable.

3. This theory is based on the energy method and involves a number of approximations, some rather rough. Factors have been introduced to correct as much as possible for the errors involved in the method, and the principal effects of the many variables involved have been considered in a reasonably

*Chance Vought Aircraft and Illinois Institute of Technology. This paper was prepared as a report for Waco Aircraft Company.

rational manner. The theory checks closely with previous theories for numerous widely divergent special cases, and there is good reason to believe that it will give reasonably accurate and conservative results in the other cases. Such experimental checks as are available confirm this belief. The theory covers many important practical cases for which no other theoretical method is available, and for such cases presumably must serve until more refined analyses are developed. Even the alternative of making and testing small portions of the structure is open to serious questions, as is discussed in paragraph 13.

4. In the following, the case of a complete cylinder is considered to be a special case of a panel. The few ways in which a cylinder must be treated differently from a panel are pointed out in their proper places.

APPLICATION OF THEORY

5. This is a theory of elastic stability and, like other such theories, assumes a construction with no imperfections of shape or elasticity. Two factors, K_1 and K_2, however, are presented, which can be applied to the results of the theory and which approximately allow for the limitations in the elasticity and strength of actual materials and the other imperfections present in actual structures.

6. As to edge or boundary conditions, the theory is first set up for the case of hinged or "simply supported" edges. However, modifications in the method of applying the theory are presented which permit any degree of fixity between hinged and fixed conditions to be evaluated, and its most important effects to be considered.

7. It seems to be common practice, probably because of the difficulty of considering these subjects, to neglect both the unfavorable effect of imperfections and the favorable effect of any end fixity which may be present. These two effects do act in opposite directions; however, particularly in dealing with curved sheets, it is not safe to assume that they cancel each other, as each may vary over a very wide range and are each functions of entirely different conditions. It is recommended that these effects should be neglected only when the product K_1 by K_2 is greater than 0.8 and there is obviously a considerable degree of end fixity present. To use

the factors K_1 and K_2 and neglect end fixity is in many cases very much overconservative, and it is believed that by far the most reliable results can be obtained by considering all these factors by the methods to be described.

8. As stated, the theory is a stability or buckling theory and does not consider the rise in resistance which may occur in thin flat panels after buckling has occurred, owing to piling up of compressive forces near the relatively stable edges, or the development of a diagonal tension field in shear.

9. The theory is developed for the case of stresses which are constant over the panel, and the question will arise as to how it can be applied to cases where these stresses are variable. If no more accurate theory is available, the following methods are suggested:

10. If the stresses vary only slightly, assume them to be constant and of their average magnitude, or of the magnitude:

$$\frac{3 S_{av} + S_{max}}{4} \qquad (1)$$

where S_{av} is the average and S_{max} is the maximum stress of each kind on that panel. (It is obviously unnecessarily conservative to use the maximum stress; and, as the average stress might give somewhat unconservative results in certain cases, the above is suggested as an arbitrary but reasonable compromise.)

11. When the stresses vary widely, study the case of the whole panel and of various portions of it, each considered as a smaller panel with a hinged edge along the artificial dividing line. Consider each of these panels to be subjected to uniform stresses of the magnitude given by equation (1). Then discard all the cases except the one which proves to be most critical. Figure 1 shows the case of a shear web of a beam. In figure 1a S_s and S_c are the equivalent uniform shear and compressive stresses assumed to be acting over the whole web. Figures 1b and 1c similarly show the uniform stresses assumed to be acting over portions of the web considered as separate panels. Judgment and experience usually indicate the cases which are likely to be critical.

12. In the buckling of curved sheets not only the condition of restraint at the boundaries against lateral and rotational displacements but also against displacements in the plane of the sheet must be considered. In this theory, it is assumed that all linear restraints are the same as if each panel were a part of a large cylinder which is divided into many such panels, the buckling deflection of which has nodes along the dividing lines. This corresponds closely to the condition of panels in actual stiffened monocoque construction, in which longitudinal and circumferential stiffeners strongly resist lateral deflections, but are incapable of interfering appreciably with displacements in the plane of the sheet (because the sheet is obviously far stiffer in this direction than any stiffener can be).

13. This kind of restraint is not the same as that existing when separate panels are loaded in grooves in testing machines. Hence the results of tests of this kind will not necessarily check with this theory, and a question should be raised concerning the common practice of applying such results to the panels of stiffened monocoque construction. All this is quite aside from the question of the lateral and rotational edge restraints usually provided in such tests. It might be stated in this connection that the conditions in a "flat end" test are indeterminate, but in most cases probably much closer to fixed end than to hinged end conditions, and hence unconservative for use in most applications. Preferable methods of testing are discussed in the appendix (paragraph 136).

14. The question of the boundary restraint in the plane of the sheet is unimportant in the buckling of flat panels but it is probably important, though usually neglected, in connection with the ultimate strength of thin flat panels, as the panels are then in the "large deflection" range.

EVALUATION OF THE ELASTIC PROPERTIES OF THE SHEET

15. In applying the theory it is necessary to first calculate certain dimensionless quantities describing the elastic properties of the sheet. For plywood sheets, we first set down the following properties of the wood alone. These can be obtained from reference 1, pages 13, 14, and 18. The symbols E_L, G_{LT}, and so forth, are as used in this reference:

16. $E = E_L$ is the compression modulus, in the direction of the grain, of the face-ply material. This may be taken as about 10 percent greater than the values of bending modulus given in reference 1, page 14. Shear strains are probably nearly as important in the buckling of plywood sheets as in the standard wood-bending test. However, a little increase over the bending value is justified because of the decrease in thickness and consequent increase in density which usually takes place in the molding of plywood, and because the compression modulus of wood, which is dominant in a stability problem, is probably somewhat larger than the tensile or bending modulus. Since an allowance has been made for scatter in the values given in this reference, the results of using them in this theory will evidently also be corrected to some extent for scatter.

$$\begin{aligned}
\mu &= \mu_{TL} \quad \text{for rotary cut veneer} \\
&= \mu_{RL} \quad \text{for quarter sliced veneer} \\
e &= (E_T/E_L) \quad \text{for rotary cut} \\
&= (E_R/E_L) \quad \text{for quarter sliced} \\
\epsilon &= E/(1 - \mu^2/e) \\
g &= G_{LT}/\epsilon = (1 - \mu^2/e)(G_{LT}/E_L) \quad \text{for rotary cut} \\
&= G_{LR}/\epsilon = (1 - \mu^2/e)(G_{LR}/E_L) \quad \text{for quarter sliced} \\
H &= 2\mu + 4g
\end{aligned} \tag{2}$$

17. The following constants depend on both the material and distribution of plies. For standard plywood (having plies laid symmetrically about the midplane and at right angles to each other) and if all plies are of the same material:

$$\begin{aligned}
A &= (1 - t_1 + t_2 - t_3 + \ldots) + e\,(t_1 - t_2 + t_3 \ldots) \\
B &= e\,(1 - t_1 + t_2 - t_3 + \ldots) + (t_1 - t_2 + t_3 \ldots) \\
C &= (1 - t_1^3 + t_2^3 - t_3^3 + \ldots) + e\,(t_1^3 - t_2^3 + t_3^3 \ldots) \\
D &= e\,(1 - t_1^3 + t_2^3 - t_3^3 + \ldots) + (t_1^3 - t_2^3 + t_3^3 \ldots)
\end{aligned} \tag{3$_1$}$$

A and B are proportional to the extensional stiffnesses, and C and D to the bending stiffnesses of the sheet in the direction of the face grain and the perpendicular direction, respectively. Obviously $A + B = C + D = 1 + e$ for this case. The numbers t_1, t_2, and so forth, are the ratios, to the outside thickness t, of the thickness with the outer plies removed, then with the next plies removed, and so forth, as in figure 2.

18. For standard plywood having plies of different woods, an average value for the different materials can be used for μ, e, g, and H without serious error, and

$$
\begin{aligned}
A &= [(1 - t_1) + (t_2 - t_3)E_{23}/E + \ldots] + e\,[(t_1 - t_2)E_{12}/E + \ldots] \\
B &= e\,[(1 - t_1) + (t_2 - t_3)E_{23}/E + \ldots] + [(t_1 - t_2)E_{12}/E + \ldots] \\
C &= [(1 - t_1^3) + (t_2^3 - t_3^3)E_{23}/E + \ldots] + e\,[(t_1^3 - t_2^3)E_{12}/E + \ldots] \\
D &= e\,[(1 - t_1^3) + (t_2^3 - t_3^3)E_{23}/E + \ldots] + [(t_1^3 - t_2^3)E_{12}/E + \ldots]
\end{aligned}
\qquad (3_g)
$$

where E_{23} is the value of E for the material of the pair of plies lying between t_2 and t_3, and so forth.

19. If materials having widely different values of μ, e, and so forth, are combined, or if the plies are symmetrical about the middle plane of the plywood but not at right angles to each other, calculate values of $M \ldots Y$, $D_1 \ldots D_6$, (equation 4) for each pair of plies such as the pair between t_i and t_j, designating them by $M_{ij} \ldots Y_{ij}$, $D_{1ij} \ldots D_{6ij}$. In doing this, take $A = C = 1$, $B = D = e$, use values of e, μ, g, and H corresponding to the material of the ply, and take θ as the angle between the grain of that ply and side b of the panel, as in figures 3a, b. Then for the whole plywood

$$
M = \Sigma(t_i - t_j)(E_{ij}/E)M_{ij}, \ldots\ldots\ Y = \Sigma(t_i - t_j)(E_{ij}/E)Y_{ij}
$$

$$
D_1 = \Sigma(t_i^3 - t_j^3)(E_{ij}/E)D_{1ij}; \ldots\ D_6 = \Sigma(t_i^3 - t_j^3)(E_{ij}/E)D_{6ij}
$$

the summation being taken over all the pairs of plies and the core ply.

20. If the plies are not symmetrical and not at right angles, proceed as for the last case, studying each ply separately and treating it as if it and its mirror image in the middle plane of the plywood formed a pair of plies like the previous one. Then, to correct for having considered the images, which do not really exist, the final values of M, N, ... D_1 ... should be divided by 2.

21. For a sheet of isotropic material of modulus E, Poisson's ratio μ, and thickness t, the above constants become

$$e = A = B = C = D = 1; \quad \epsilon = E/(1 - \mu^2); \quad g = (1 - \mu)/2, \quad H = 2 \quad (3_3)$$

22. For applying the theory to the general case of any kind of a sheet, see the appendix, paragraph 90.

23. All the quantities of equations (2) and (3) are independent of the orientation of the sheet in the panel. The following constants depend also on the angle θ of the principal elastic axis of the sheet (the outer ply grain direction for standard plywood) with the shorter side of the panel b (figs. 3a, b). These constants are, however, independent of the dimensions and loading of the panel.

24. All the constants needed for the most general case are given below, but only about half of them are required for the average problem. In equation (5) the quantities in braces are zero for the common cases of isotropic sheets, all 0° and 90° plywood panels, and all "balanced" 45° plywood panels. They may always be neglected if X and Y are less than 0.02. The quantities A_1 ... A_6 are used only in case A problems, and the quantities B_1 ... B_5 only in case B problems. All the quantities except D_1 ... D_6 define extensional properties of the sheet, which are required only when there is curvature. The quantities D_1 ... D_6 define flexural properties, which are required for flat sheets as well as for curved.

$$M = 4\,[A \sin^4\theta + B \cos^4\theta + H \sin^2\theta \cos^2\theta]$$

$$N = 4\,[B \sin^4\theta + A \cos^4\theta + H \sin^2\theta \cos^2\theta]$$

$$P = 4\,[(A + B - H) \sin^2\theta \cos^2\theta + \mu]$$

$$Q = 4\,[(A + B - H) \sin^2\theta \cos^2\theta + g]$$

$$X = 2 \sin\theta \cos\theta\,[2A \cos^2\theta - 2B \sin^2\theta + H(\sin^2\theta - \cos^2\theta)]$$

$$Y = 2 \sin\theta \cos\theta\,[2A \sin^2\theta - 2B \cos^2\theta - H(\sin^2\theta - \cos^2\theta)]$$

$$D_1 = 0.82\,[C \sin^4\theta + D \cos^4\theta + H \sin^2\theta \cos^2\theta] \qquad (4)$$

$$D_2 = D_3 = 0.82\,[D \sin^4\theta + C \cos^4\theta + H \sin^2\theta \cos^2\theta]$$

$$D_4 = 0.82\,[6(C + D - H) \sin^2\theta \cos^2\theta + H]$$

$$D_5 = 0.82 \sin\theta \cos\theta\,[2C \cos^2\theta - 2D \sin^2\theta + H(\sin^2\theta - \cos^2\theta)]$$

$$D_6 = 0.82 \sin\theta \cos\theta\,[2C \sin^2\theta - 2D \cos^2\theta - H(\sin^2\theta - \cos^2\theta)]$$

These expressions simplify a great deal for particular values of θ. For $\theta = 0^\circ$

$$M = 4B;\ N = 4A;\ P = 4\mu;\ Q = 4g;\ X = Y = 0$$

$$D_1 = 0.82D;\ D_2 = D_3 = 0.82C;\ D_4 = 0.82H;\ D_5 = D_6 = 0 \qquad (4_{0^\circ})$$

For $\theta = 90^\circ$

$$M = 4A;\ N = 4B;\ P = 4\mu;\ Q = 4g;\ X = Y = 0$$

$$D_1 = 0.82C;\ D_2 = D_3 = 0.82D;\ D_4 = 0.82H;\ D_5 = D_6 = 0 \qquad (4_{90^\circ})$$

For $\theta = 45^\circ$

$$M = N = A + B + H;\ P = A + B - H + 4\mu$$

$$X = Y = A - B;\ Q = A + B - 2\mu \qquad (4_{45^\circ})$$

$$D_1 = D_2 = D_3 = 0.206\,(C + D + H);\ D_4 = 1.23\,(C + D) - 0.41H$$

$$D_5 = D_6 = 0.41\,(C - D)$$

For an isotropic sheet

$$M = N = 4;\ P = 4\mu;\ Q = 2(1 - \mu);\ X = Y = 0 \qquad (4_{iso})$$
$$D_1 = D_2 = D_3 = 0.82;\ D_4 = 1.65;\ D_5 = D_6 = 0$$

25. The values of M, N, P, Q, X, and Y thus found are then used to compute whichever of the following quantities are needed in the problem being studied:

$$A_1 = MQ^2 - \left\{QY^2\right\};\ A_2 = P^2Q - \left\{NY^2\right\};\ A_3 = MNQ - P^2Q$$
$$\left\{A_4 = MQX - XY^2;\ A_5 = PXY - MX^2;\ A_6 = PQY - MQX\right\}$$
$$B_1 = A_3;\ B_2 = MN^2 - NP^2 + NQ^2 + \left\{4NXY - 4PX^2 - QX^2\right\};$$
$$B_3 = N^2Q - \left\{NX^2\right\} \qquad (5)$$
$$\left\{B_4 = NQX - NPX + N^2Y - X^3;\ B_5 = MNX - PQX - P^2X + NQY\right\}$$
$$C_1 = MQ;\ C_2 = (P + Q)^2 + \left\{4XY\right\};\ C_3 = NQ;\ C_4 = MN - P^2 - 2PQ$$
$$\left\{C_5 = QX + NY;\ C_6 = -X^2;\ C_7 = NY - 2PX - QX;\ C_8 = MX + QY\right\}$$

CALCULATION OF STABILITY STRESSES, HINGED EDGES

26. After calculating the previous sheet properties, which can then be used for panels of any dimensions and curvature, the stability stresses are analyzed. To reduce confusion, four types of problems are considered: case A, for unstiffened cylinders or panels with the longer sides a curved; case B, for unstiffened panels with the shorter sides b curved; and cases A' and B' for similar stiffened cylinders and panels. For all these cases

$$F_a = K_1K_2S_a;\ F_b = K_1K_2S_b;\ F_s = K_1K_2S_s \qquad (6)$$

where

S_a, S_b, and S_s theoretical compressive stresses in the directions of a and b, respectively, and the shear stress which will cause instability under ideal conditions

F_a, F_b, and F_s corresponding stresses which can be expected to cause failure in practical construction

27. Quantity K_1 (fig. 6) allows for the limited strength of the material and other imperfections in flat sheets. In this figure $S_{theor\ stab}$ is the theoretical stability stress S_a, S_b, or S_s; $S_{mat\ strength}$ is the corresponding strength of the material under these types and directions of stress, that is, the crushing strength in the a direction, the crushing strength in the b direction, and the shearing strength in the a or b direction.

28. In some cases, a composite material is involved, for example, a sheet with stiffeners in the a direction. For this case, there are two values of S_a, one for the sheet and one for the stiffener (as discussed later). In such cases the value of K_1 for all the materials should be determined and the lowest value used with all of them. Some data on the crushing and shear strength of plain woods and plywood panels are given in reference 1 (pp. 14, 30, 38, and 41).

29. Quantity K_2 (fig. 7) allows for the additional effect of imperfections in curved sheets. In this figure a and t are the length of the curved side and thickness of the panel, while t' is a rough "effective thickness" for stiffened construction, to be used in studying buckling across stiffeners. The values of m and n used are the critical values, corresponding to the final values of S_a, S_b, or S_s, as discussed in the following.

CASE A

30. For unstiffened cylinders, and the buckling between stiffeners of panels with their longer sides a curved (or with equal sides). For this case, shown in figure 5a, the stability condition is

$$s_a S_a + s_b S_b + s_s S_s = S \frac{m^2}{\lambda} \left[\frac{\Sigma A_i a_i}{\Sigma C_i c_i} \left(\frac{\alpha}{mn} \right)^2 + \Sigma D_i d_i \right] \quad (7a)$$

where

$$S = \epsilon\left(\frac{t}{a}\right)^2, \quad \alpha = \frac{ab}{2\pi rt}\left(= \frac{b}{t} \text{ for cylinder}\right) \qquad (8)$$

and $\lambda = 1$ for cylinders and is given by figure 5 for panels, λ being a correction factor allowing for the fact that, at the panel ends b the nodes must really be vertical (instead of inclined, as shown in the figure and as assumed in developing the theory). The A's, C's, and D's are the sheet properties previously defined. The s's, a's, c's, and d's are functions (fig. 9, or appendix, par. 114) of:

$$\beta = \frac{bm}{an} \qquad (9)$$

(which obviously represents the ratio between the half wave lengths of the buckles in the b and a directions) and of γ, the tangent of the angle made by the buckling waves with the sides b (fig. 3a). The s's, a's, and so forth, can be found for any value of β and γ from figure 9 at the end of this report, the use of which is explained in figure 8 and in the example given later (par. 67).

31. For flat panels, the radius r is infinite and hence $\alpha = 0$. The right-hand side of equation (7a) then reduces to $S(m^2/\lambda)\Sigma D_i d_i$.

32. Either the ratios between stresses S_a, S_b, and S_s, or all but one of them, will be known; in any case the magnitude of one of them is the desired unknown. Everything else involved in equation (7a) will be known except for the angle of the waves, defined by γ, and the number of half waves in the a and b directions m and n. These must be determined to make the unknown stability stress a minimum. The usual method of doing this is to set the derivatives of this stress with respect to γ, m, and n equal to zero and use these relations to eliminate γ, m, and n from equation (7a).

33. However, when so complex a relation is involved this proves to be impractical. The only way in which the problem can be solved, therefore, seems to be to try various

values of γ, m, and n in equation (7a) until the values which make the stability stress a minimum have been found. This is laborious but by systematizing the work, as will be demonstrated, it is quite practicable.

34. In most problems γ varies between 0.75 and −0.75, and it is sufficient to consider the values 0, ± 0.25, ± 0.50, and ± 0.75 (adding ± 1 for extreme cases, such as when combinations of shear and tension are present) as in figure 9. For each value of m and n, therefore, these four values of γ would be tried (the plus and minus values can be dealt with together in most of the work) and the smallest of the values of stress found would be selected; or, more accurately, the stress would be plotted against γ and the low point of the curve used.

35. The numbers m and n can be only whole numbers. In the case of panels, they can have any value except zero — that is,

$$m = 1, 2, 3, \ldots; \quad n = 1, 2, 3, \ldots \qquad (10_{panel})$$

Combinations of m and n, such as 1, 2; 1, 1; 2, 1; and so forth, therefore would be tried, using larger and larger values as long as the resulting stress decreases, but stopping as soon as it starts to increase. In the case of small panels, it is usually found that the combination 1, 1 gives values smaller than 1, 2 or 2, 1; it is then unnecessary to go any further, the values of 1, 1 being accepted as the answer.

36. In the case of very large panels, the critical values of m and n may be fairly large and so it might take a long time to reach them by studying every combination. In some cases the approximate number of waves will be known by previous experience. Rough approximations also might be used to determine the approximate number — for instance, it can be shown that m and n will usually be of the same general order of magnitude as $\sqrt[4]{\frac{M}{D_1}}\frac{0.1a}{\sqrt{rt}}$ and $\sqrt[4]{\frac{N}{D_2}}\frac{0.1b}{\sqrt{rt}}$. However, the following method will generally be found as simple and quick as any: the dots in figure 4a

represent various combinations of m and n. Now in order to be sure that any combination gives a minimum stress, the next combination in all possible directions must give a higher value of stress. Thus in figure 4b any of the encircled combinations would be critical if the dotted ones adjacent to it all give higher stresses than it does. If two such combinations are found, as sometimes occurs, both, of course, must be evaluated and and the lower stress chosen.

37. To locate such critical combinations, start with the combination at the origin (1,1) and try combinations along both the m and n axes, continuing along each axis as long as the resulting stress decreases, but stopping just as soon as it starts to increase. The low point thus found will usually be a critical point, but to check this, proceed from this low point at right angles to the axis until the stress again starts to rise. At the low point thus reached, branch off again at right angles until a "boxed in" point, such as in figure 4b, is finally reached. This process might be likened to the flow of a river in rolling country — it flows along any downward path which it meets until it arrives at a depression without any outlet, where it forms a lake, corresponding to our critical point.

38. In an extreme case this process might involve the investigation, successively as indicated by the arrows, of the combinations shown by dots in figure 4c; this results in the location of the two encircled critical combinations, one of which will produce the lowest stress of any possible combination. In the case of very large panels it may pay to skip some of the points — say by making about equal steps along the logarithmic scale of figure 4, from (1,1) to (2, 1) to (4, 1) to (8, 1) to (16, 1), and so forth,— until the low point has been approximately located. Practical problems will probably never require as complicated a search as that shown in figure 4c. Most problems will require investigation of from 3 to 10 combinations, each taking a half hour or less of time, to determine all critical combinations of compression and shear for a given panel.

39. In the case of a complete cylinder, if a is taken as the circumference ($a = 2\pi r$), the number m must be even, and can be zero. That is, for this case

$$m = 0, 2, 4, 6\ldots; \quad n = 1, 2, 3\ldots \qquad (10_{cyl})$$

For the case when $m = 0$ (which represents buckling into a symmetrical shape like a sylphon bellows), the following simple solution can be used:

If

$$m = 0: \quad S_a = S_s = \infty$$

$$n = \sqrt{\frac{b^2}{at}\sqrt{\frac{A_3}{C_3 D_2}}};$$

Then if (11)

$$n < 1, \quad S_b = S\left(\frac{\alpha^2 A_3}{C C_3} + \frac{a^2}{b^2} D_2\right)$$

while if

$$n > 1, \quad S_b = 2S \frac{a}{t} \sqrt{\frac{A_3 D_2}{C_3}}$$

For other values of m the same procedure as for panels must be used, trying various combinations of m and n such as 2, 2; 2, 1; 4, 1; and so forth, as previously discussed.

CASE B

40. For buckling between stiffeners of panels with their shorter sides b curved:- For this case figure 3b should be followed. Otherwise the only change from the procedure described for case A is that B_1, B_2... and b_1, b_2... must be substituted for A_1, A_2... and a_1, a_2.... Equation (7a), therefore, changes to

$$s_a S_a + s_b S_b + s_s S_s = S \frac{m^2}{\lambda}\left[\frac{\Sigma B_i b_i}{\Sigma D_i c_i}\left(\frac{\alpha}{mn}\right)^2 + \Sigma D_i d_i\right] \quad (7b)$$

CASES A' AND B'

41. For buckling across stiffeners:- It is necessary to consider not only the possibility of buckling of the panels between

stiffeners, but also the possibility of buckles occurring across both longitudinal and circumferential stiffeners. This is most likely to occur under a compressive stress in the direction of the stiffeners, but it can also occur under any type of stress, and is frequently the condition determining the design of the stiffener.

42. The treatment of these problems is the same as for cases A and B with the following exceptions: For buckling across stiffeners which run in the direction of sides a: Instead of studying various combinations of $m = 1, 2, 3, \ldots$ with $n = 1, 2, 3, \ldots$, take $n = 1$ and study combinations of $m = 1, 2, 3, \ldots$ with $b = 2b', 3b', 4b', \ldots$, b' being the spacing of the stiffeners. Then take $\lambda = 1$, and substitute

$$\left(1 + \frac{E_a'A_a'}{E_a t b'}\right) S_a$$

for S_a, and add

$$\frac{4E_a'A_a'}{\epsilon t b'}$$

to the previous expression for M,

$$\left(1 + \frac{h_a^2/\rho_a^2}{1 + \frac{E_a'A_a'}{E_a t w_a}}\right) \frac{\pi^2 E_a'A_a'\rho_a^2}{\epsilon t^3 b'} \qquad (12)$$

to the previous expression for D_1,

$$\frac{\pi^2 G_a' J_a'}{\epsilon t^3 b'}$$

to the previous expression for D_4.

43. For the case of simple stiffeners (made of one material) E_a' is the compressive modulus of elasticity of the stiffener material in the direction of its length. For wood, it may be taken about 5 percent greater than the bending modulus given in reference 1 (p. 14) since the modulus of wood in compression is probably higher than in tension or bending, as previously mentioned.

44. The effective compressive modulus of the panel in the direction of side a is E_a. Methods of determining it are discussed later in this section.

45. The cross sectional area of the stiffener alone is A_a', while h_a is the distance from the center of gravity of the stiffener alone to the middle surface of the panel; ρ_a is the radius of gyration of the stiffener alone about its centroidal axis parallel to the panel; w_a is the total "effective width" of panel which can be considered to act with the stiffener in bending (not to be confused with other kinds of effective widths), and may be taken as

$$w_a = b' \tag{12'}$$

or

$$w_a = \frac{aQ}{mM^*}$$

whichever is the smaller.

46. The torsional stiffness of the stiffener combined with any portion of the sheet which may form with the stiffener a tubular section is denoted with $G_a'J_a'$; it can be computed by standard methods of mechanics, for example, see reference 4, part I (p. 270) and part II (p. 279).

47. Built-up stiffeners, made of more than one material, can first be converted to equivalent simple stiffeners, or if preferred the quantities $E_a'A_a'$, $E_a'A_a'\rho_a^2$, and $G_a'J_a'$ can be taken as the total longitudinal, bending and torsional stiffnesses of the complete stiffener.

48. For buckling across stiffeners which run in the direction of sides b: Take $m = 1$ and study combinations of $n = 1, 2, 3, \ldots$ with $a = 2a', 3a', 4a', \ldots$ where a' is the spacing of these stiffeners. Also take $\lambda = 1$, and substitute

---

*The value of M given by equation (4) should be used, without the added term of equation (12).

$$\left(1 + \frac{E_b'A_b'}{E_b t a'}\right) S_b$$

for S_b and add

$$\frac{4E_b'A_b'}{\epsilon t a'}$$

to the previous expression for N

$$\left(1 + \frac{h_b^2/\rho_b^2}{1 + \frac{E_b'A_b'}{E_b t w_b}}\right) \frac{\pi^2 E_b'A_b'\rho_b^2}{\epsilon t^3 a'} \qquad (13)$$

to the previous expression for D_2

$$\frac{\pi^2 G_b'J_b'}{\epsilon t^3 a'}$$

to the previous expression for D_4

where:

$$w_b = a', \qquad (13')$$

or

$$w_b = \frac{bQ}{nN^*}$$

whichever is the smaller.

and the other quantities have similar definitions to those mentioned above, merely interchanging a and b.

49. To study the possibility of buckles crossing both the longitudinal and transverse stiffeners, combine the above changes. That is, take $m = n = 1$ and study combinations of $a = 2a', 3a', 4a', \cdots$ with $b = 2b', 3b', 4b', \cdots$ and make all the substitutions of equations (12) and (13) (adding both terms to D_4).

*Use N without the added term of equation (13).

50. The values of S_a and S_b obtained by this method are, as before, the stresses in the sheet when buckling occurs. The corresponding stresses in the stiffeners, designated by S_a' and S_b', of course would be, respectively, E_a'/E_a and E_b'/E_b times as great.

51. Values of E_a and E_b for 0° and 90° plywood are given in reference 1 (p. 41). Materials like 45° plywood are very sensitive to the amount of restraint against lateral expansion or contraction (say to stiffeners running in the lateral direction). Methods for calculating the effective moduli of plywood under various conditions are given in reference 1. It can be shown that for ordinary 45° plywoods, assuming that the lateral stiffeners have the same effect as if their area were uniformly distributed

$$E_a = \frac{4\epsilon}{1/g + Q/AB - \dfrac{(1/g - Q/AB)^2}{1/g + Q/AB + \dfrac{4\epsilon t a'}{E_b' A_b'}}} \qquad (14)$$

with the same formula for E_b except that a and b are interchanged (in the last sub-fraction).

52. In all the foregoing calculations the same rules must be followed as for cases A and B, that is, the symbols a and b are to be used so that $a > b$, and figure 3a and equation (7a) are to be followed when a is the curved side, while figure 3b and equation (7b) are to be followed when b is the curved side.

CONSIDERATION OF EDGE FIXITY

53. The most important effects of edge fixity along the sides a can be considered by simply multiplying D_a by

$$\Delta_a = \left(\frac{1 + \frac{n+1}{n}\Delta_a}{1 + \Delta_a}\right)^2, \quad \text{where} \quad \Delta_a = \frac{K_a + \pi^2 G_a'' J_a'' b m^2}{D_a \epsilon t^3 a^2 n} \qquad (15a)$$

Δ_a is a measure of the fixity of the sides a and has a value of zero for hinged edges and infinity for fixed edges, which would give values of Φ_2 of 1 and $(1+1/n)^2$, respectively. For intermediate fixities, the approximate formulas of equation (15a) can be used.

54. In these expressions $G_a''J_a''$ is the torsional stiffness of the stiffener or other member to which the panel is attached along each side a. A measure of any distributed elastic resistance to rotation which may be present along each side a is denoted by K_a, measured as the elastic resisting moment per radian of rotation, per unit length of the edge. Such a distributed elastic resistance might be produced, for instance, by closely spaced wing rib members running between the edges a and the other face of the wing; for such a case K_a could be taken as three times the bending stiffness of each cross member, divided by their length and by their spacing.

55. The value of Δ_a given by equation (15a) is for the case when each edge member separates and is attached to two similar and similarly loaded panels; if the member is attached to only one panel, then twice the above value should be used. If the two edges a of the panel have different fixities, then Δ_2 may be taken as the average of its values for each of the two edges.

56. Similarly, to consider the edge fixity along side b, multiply D_1 by

$$\Phi_1 = \left(\frac{1 + \frac{m+1}{m}\Delta_b}{1 + \Delta_b}\right)^2, \quad \text{where} \quad \Delta_b = \frac{K_b + \pi^2 G_b'' J_b'' a n^2}{D_1 \epsilon t^3 b^2 m} \qquad (15b)$$

The various quantities involved have similar definitions to those of equation (15a), merely interchanging 1 and 2, a and b, and m and n.

57. To consider edge fixities along both sides a and b, combine the above changes.

SPECIAL CASE OF COMPRESSIVE LOADING OF SYMMETRICAL STRUCTURES

58. The foregoing methods simplify a great deal when applied to certain special cases. One of the most common of such

cases is that of compressive loading of cylinders or panels having a principal elastic axis in the direction of the compression, for example, 0° or 90° plywood with or without longitudinal and circumferential stiffeners.

59. For this case $\gamma = 0$ from symmetry, and hence $\lambda = 1$, and cases A and B become identical except for differences in symbols. Using the symbols of case A (fig. 3a), but now without any limitation that a must be greater than b, it is found (from equation (7a')) by dropping the term $0.03\beta^4 D_1$, which is not required and has negligible effect in this case) that:

$$S_b = \frac{\epsilon t}{2\pi r}\left[\frac{A_3}{C_1\beta^2+C_3/\beta^2+C_4}\,\frac{a^2}{2\pi r t m^2} + (D_1\beta^2+D_2/\beta^2+D_4)\frac{2\pi r t m^2}{a^2}\right] \tag{16}$$

60. If the conditions for minimizing the buckling stress are set up: namely, $\partial S_b/\partial\beta^2 = \partial S_b/\partial m^2 = 0$, they can be solved in this case, and the following can be obtained as the values which m, n, and β would have if m and n did not have to be integers:

$$\beta'^2 = \frac{C_3D_1 - C_1D_2}{C_1D_4 - C_4D_1} - \sqrt{\left(\frac{C_3D_1 - C_1D_2}{C_1D_4 - C_4D_1}\right)^2 + \frac{C_3D_4 - C_4D_2}{C_1D_4 - C_4D_1}}\,;$$

$$m'^2 = \frac{a^2}{2\pi r t}\sqrt{\frac{A_3}{(C_1\beta'^2+C_3/\beta'^2+C_4)(D_1\beta'^2+D_2/\beta'^2+D_4)}}\,;\quad n'^2 = \frac{b^2}{a^2\beta'^2}m'^2 \tag{17}$$

The buckling stress S_b can then be obtained from equation (16) by taking m and n as the integers (such as given in equations (10) pars. 35 and 39) which are nearest to the values of m', n' given by equation (17), and taking $\beta = bm/an$.

EXAMPLE

61. The foregoing description of the method of applying this theory doubtless gives an impression of great complexity, a good deal of which is ascribable to the effort

to keep it as general as possible. To clarify the method and show that it is practical to apply, a typical problem involving a medium sized plywood panel is completely worked out in the following. Figure 10 shows the details of the construction. Using equations (2) (par. 16) and reference 1 (pp. 14 and 18) it is found for quarter sliced mahogany that

$$E = 1.10 \times 1{,}260{,}000 = 1{,}390{,}000 \text{ lb/sq in.}$$

$$\mu = 0.024; \quad e = 0.078; \quad 1 - \mu^2/e = 0.99 \qquad [2]$$

$$\epsilon = 1{,}390{,}000/0.99 = 1{,}400{,}000; \quad g = 0.99 \times 0.049^* = 0.049$$

$$H = 2 \times 0.024 - 4 \times 0.049 = 0.243$$

62. The quantity $1 - \mu^2/e$ varies from about 0.99 for soft woods to about 0.97 for hard woods, and hence might be taken as unity for wooden construction. The numerical calculations involved in applying this theory are not critical; and since the data will seldom be known to closer than a few percent, slide rule accuracy, with no more than three significant figures retained, is all that is required or justified in these calculations.

From equations (3):

$$A = (1 - 0.646 + 0.156) + 0.078\,(0.646 - 0.156) = 0.548$$

$$B = 0.078\,(1 - 0.646 + 0.156) + (0.646 - 0.156) = 0.530 \qquad [3]$$

$$C = (1 - 0.646^3 + 0.156^3) + 0.078\,(0.646^3 - 0.156^3) = 0.756$$

$$D = 0.078\,(1 - 0.646^3 + 0.156^3) + (0.646^3 - 0.156^3) = 0.322$$

BUCKLING BETWEEN STIFFENERS

63. For buckling of the panel between stiffeners, since the curved side is the shorter, case B, as shown in

*This value of G_{LR}/E_L given in reference 1 (p. 18) is used here for consistency. It should be mentioned, however, that there is evidence that it should really be 20 to 30 percent higher. This would considerably change some of the following computations.

figure 10e is used. Since $\theta = 45^\circ$ equations (4_{45°) (par. 24) can be used

$$M = N = 1.078 + 0.243 = 1.32; \quad X = Y = 0$$

$$P = 1.078 - 0.243 + 4 \times 0.024 = 0.93$$

$$Q = 1.078 - 2 \times 0.024 = 1.03 \qquad [4]$$

$$D_1 = D_2 = D_3 = 0.206\,(1.078 + 0.243) = 0.273$$

$$D_4 = 1.23 \times 1.078 - 0.41 \times 0.243 = 1.23$$

$$D_5 = D_6 = 0.41\,(0.756 - 0.322) = 0.178$$

From equations (5) (par. 25),

$$B_1 = (1.32^2 - 0.93^2)\,1.03 = 0.90$$

$$B_2 = (1.32^2 - 0.93^2 + 1.03^2)\,1.32 = 2.56; \quad B_3 = 1.32^2 \times 1.03 = 1.79 \qquad [5]$$

$$C_1 = C_3 = 1.32 \times 1.03 = 1.36; \quad C_2 = (0.93 + 1.03)^2 = 3.84$$

$$C_4 = 1.32^2 - 0.93^2 - 2 \times 0.93 \times 1.03 = +1.04$$

From equations (8) (par. 30) and figure 10e,

$$a = 14; \quad b = 12; \quad b/a = 0.86; \quad r = 30; \quad t = 0.19$$

$$S = 1,400,000\,(0.19/14)^2 = 260 \text{ lb/sq in.} \qquad [8]$$

$$\alpha = \frac{14 \times 12}{2\pi 30 \times 0.19} = 4.7$$

64. Edge fixity and the correction factors K_1 and K_2 need not necessarily be considered in a problem such as this, but will be here for completeness and to illustrate their effect. Considering equations (15a, b) (pars. 53 and 59) and the accompanying discussion, since there are no cross members in this construction $K_a = K_b = 0$. The shear stiffness of Douglas fir, from reference 1 (pp. 14 and 18) is approximately $0.06 \times 1,700,000 = 102,000$ pounds per square

inch, while that of 1/16 45° plywood will be nearly the same as for the panel skin, which is $Q\epsilon/4 = 1.03 \times 1400000/4 = 360,000$ pounds per square inch, approximately.

65. Then, from reference 4 (pt. I, p. 270) the torsional stiffness of each longitudinal stiffener is

$$G_a''J_a'' = [M_t/\theta = \beta bc^3 G] = 0.229 \times 0.875 \times 0.438^3 \times 102,000 = 1710 \text{ lb in}^2 \qquad (A)$$

(the notation in the brackets is that of the reference). From reference 4 (pt. II, p. 279) that of the circumferential stiffeners is

$$G_b''J_b'' \left[= M_t/\theta = \frac{4A^2}{\int_0^s \frac{ds}{Gh}} \right] = \frac{4(3 \times 0.69)^2}{\frac{2 \times 3}{360000 \times 0.063} + \frac{2 \times 0.69}{102000 \times 0.44}}$$

$$= 58,000 \text{ lb in}^2 \qquad (B)$$

and from equations (15a, b)

$$\Delta_a = \frac{\pi^2 \times 1710 \times 12\, m^2}{0.273 \times 1400000 \times 0.19^3 \times 14^2 n} = 0.40 \frac{m^2}{n}$$

$$\Delta_b = \frac{\pi^2 \times 57600 \times 14\, n^2}{0.273 \times 1400000 \times 0.19^3 \times 12^2 m} = 21.2 \frac{n^2}{m} \qquad [15]$$

66. The solution of the stability equation (7b) (par. 40) is most conveniently carried out in the tabular form of table I, and to save time as much as possible of the table is filled in at one time. Each column of the table represents a solution of the equation for one combination of m, n, and γ. The quantities in the different rows are defined at the left of the table, so that the table is nearly self-explanatory. However, discussion of some points is advisable.

67. The charts of figure 9 (see back-cover pocket) can be used not only to obtain the a's, b's, s's, and so forth, but owing to their logarithmic scale, products such as A_1a_1, B_3b_3, and so forth, and quotients such as $"S+"/S_s$, $"S-"/S_b$, and so forth, are obtained directly from them. Proper use of these charts greatly facilitates the work, and contributes more than anything else to make this method usable.

68. A sliding scale must first be constructed, by simply cutting out the paper scale at the right of figure 9, and cementing to it a piece of heavy cardboard (such as used to back up pads of paper) as shown by the dotted lines on the scale and by figure 8a.

69. As indicated, the scale must be cut accurately along the line PP, and the side of the cardboard opposite PP must be straight and parallel to PP. The hole in the cardboard indicated in the figure helps to grip it for sliding it, as shown in figure 8b. A non-aqueous cement, such as rubber cement or the common "waterproof" cements should be used, or else only the corners of the scale cemented, so as not to distort the scale.

70. Next, spread figure 9 on a flat surface and adjust the scale on it so that one of the vertical axes of figure 9, say the one farthest to the left, is at the desired value of β, at both the top and bottom of the scale. Now, holding the scale firmly in this position with the left hand, place a triangle against the right side of the scale and a weight on top of it, as shown in figure 8a. The scale can now be moved up and down as desired, and will be properly set for this value of β for all the charts having the same vertical axis.

71. Now to find a_1 or b_2, for example, slide the scale until the horizontal axis of the corresponding chart is opposite 1 on the scale. Then read the values of a_1 or b_2 on the scale (at the intersection with the desired γ curve) as shown in figure 8b. It is a good idea to check a few readings at this point, using the relation $a_1 = b_2 = \beta^2\gamma^2$. An accuracy of within a few percent is all that can be expected with such paper scales, but as explained before this is sufficient for the purpose. It is useless to try to read the scale closer than to two or three significant figures, that is, to within 1 or 2 percent.

72. Products such as A_1a_1 are obtained in exactly the same way, except that instead of setting the horizontal axis of the chart at the point 1 on the scale, it is set at the value of A_1 on the scale. The scale readings at the intersections with the curves are then the corresponding values of A_1a_1, as shown in figure 8c. All values of γ are taken care of at one setting.

73. In this manner, the rows B_1b_1, B_2b_2, B_3b_3, C_2c_2, $(\Delta_1 D_1)d_1$ of the table are filled in before moving the sliding scale to another vertical axis. The scale is similarly adjusted on the second vertical axis to obtain $(\Delta_2 D_2)d_2$, $1.36(c_1 + c_3)$ and $0.178\ (d_5 + d_6)$, and on the third to obtain D_3d_3 (these figures are good for all values of β). Finally, it is moved to the last axis, and C_4c_4 and D_4d_4 are taken care of.

74. After completing the various intermediate operations in the table, which are clearly indicated, the values $S+$ and $S-$ are obtained, representing the right hand side of equation 7b for positive and negative values of γ, respectively. The last five rows of the table, which represent various stress combinations causing buckling, can then be filled in with the last setting of the scale, on the fourth axis. This involves division, which is carried out as before, except that the roles of the horizontal axis of the chart and its γ curves are interchanged. For example, to obtain $S+/s_s$ the value of $S+$ is set at the desired γ curve on the s_s chart and the quotient $S+/s_s = S_s$ is read at the horizontal axis, as shown in figure 8d.

75. Ordinarily the positive shear (in the direction indicated in figs. 3a, b) required to buckle the panel is obtained from $S+$, and the shear in the negative or opposite direction required to produce buckling would be found from $S-$. The reverse is true in the present problem because the direction of the shear in figure 10e is opposite to the standard direction. The critical compression is always obtained from $S+$ or $S-$, whichever is the smaller.

76. Having filled in the table for each combination of m and n, the smallest values of the stresses in each of the last five rows are encircled, as shown, and the encircled, as shown, and the encircled values are plotted as shown in figure 11a. A smooth curve drawn through these

five points then gives a graph showing all combinations of compressive and shear stresses which can produce buckles of the shape specified by this combination of m and n (minimized as far as the angle γ is concerned).

77. Such graphs are drawn for each combination of m and n and further combinations are investigated as long as any part of the new graphs come inside those already drawn, stopping as soon as all parts of the new graph come outside those already drawn. This is in accordance with the previous discussion (par. 37) but by comparing such graphs instead of individual stresses, the minimum values of all combinations of stress which will produce buckling are simultaneously obtained. In the present case, this procedure results in figure 11b, and the minimum stress combinations are evidently given by the irregular heavy line, consisting of part of the 3, 1 graph and part of the 2, 1 graph.

78. It might be well to go back now to get a little more accurate values for the critical stress combinations shown circled in figure 11b, by plotting the stresses against the different values of γ and selecting the lowest point of the resulting curve, instead of merely picking the smallest of the stresses found for any of the γ's investigated. Such a plot is shown in figure 11c, for the point doubly encircled in figure 11b. This is an unnecessary refinement for most practical cases.

79. The stress combinations causing buckling under perfect conditions having been found, the factors K_1 and K_2 will be applied to determine the practical buckling stress combinations. (See figs. 6 and 7.) The material strength of plywood such as this, in directions 45° to the grain (which must be known to determine K_1), is not very well established. However, the following values, estimated from various sources, should not be greatly in error, and will serve at any rate to illustrate the method; shear, 3400; compression 2300; and combination of equal shear and compression, 2000 pounds per square inch each. The determination and application of K_1 and K_2 and the final results for buckling of the panel between stiffeners, are summarized in table II. "Good construction" is assumed; this category is intended to include all aircraft construction. The values of $F_{pract\ stab}$, the stress combinations which are likely to produce buckling between stiffeners in practical construction, are also plotted and connected with a dotted line in figure 11b.

80. The ability of the panel to support more shear stress in one "favorable"* direction than in the other, evidenced by the lack of symmetry about the horizontal axis of the curves of figure 11, is due to its greater bending stiffness in the direction of the face grain than in the perpendicular direction. To eliminate this unsymmetrical behavior, it is necessary that $C = D$.

81. It is of interest that both the condition $C = D$ and the condition $A = B$ (which insures a balanced plywood as far as extensional strength and stiffness is concerned) can be satisfied by two unknowns, such as t_1 and t_2 in a five-ply plywood. Using equation 3 (par. 17) in these conditions it is found that $t_1 = 0.81$ and $t_2 = 0.31$. That is, both extensional and bending balance is obtained in a five-ply plywood having 9.5 percent of its thickness in the outer plies, 25 percent in the intermediate plies, and 31 percent in the core. It can be shown that such a plywood would have about the same properties as the theoretical plywood having an infinite number of infinitesimal plies laid alternately at right angles to each other.

BUCKLING ACROSS STIFFENERS

82. Owing to the depth of the circumferential stiffeners, or bulkheads, there is no danger of buckling across them, but the possibility of buckling across the smaller longitudinal stiffeners must be considered. Since the curved side of the "panel" for such buckling would be two or more times 12 inches, and hence longer than the 14-inch straight side, as shown in figure 10f, the case A' must be used. The meanings of a and b are reversed from what they were before, a now being in the circumferential direction and b in the longitudinal, as shown.

83. The stiffeners across which buckling may occur run in the direction b; hence equations (13) and (13') (par. 48) and the discussions accompanying them are used. Then

---

*Standard 45° plywoods have the maximum buckling strength in shear when the face grain is in the direction of the diagonal compression.

$m = 1$; $n = 1, 2, \ldots$; $a' = 12$; $b' = 14$; $r = 30$; $t = 0.19$

$a = 2 \times 12, 3 \times 12, \ldots = 24, 36, \ldots$; $b = 14$; $b/a = 14/a$

$S = 1,400,000\,(0.19/a)^2 = 50000/a^2$ (equation (8), par. 30)

$$\alpha = \frac{14\,a}{2\pi 30 \times 0.19} = 0.395a$$

$E_a'A_a' = (1.05 \times 1,700,000)(2 \times 0.438 \times 0.70) = 1,090,000$ lb, roughly

$E_b'A_b' = (1.05 \times 1,700,000)(0.875 \times 0.438) = 683,000$ lb

$$E_b = \frac{4 \times 1400000}{20.4 + 3.55 - \dfrac{(20.4 - 3.55)}{20.4 + 3.55 + \dfrac{4 \times 1400000 \times 0.19 \times 14}{1090000}}}$$

$= 342,000$ lb/in.^{2} (equation (14) par. 51).

$G_a''J_a'' = 57,600$ lb in.^{2} (equation (B) par. 65)

$G_b'J_b' = G_b''J_b'' = .1710$ lb in.^{2} (equation (A) par. 65)

$\rho_b = 0.875/\sqrt{12} = 0.25$

$h_b = (0.875 + 0.19)/2 = 0.53$ in.

$w_b = \dfrac{1.03}{1.32}\dfrac{14}{n} = \dfrac{10.9}{n}$ (equation (13') (par. 48) — this is always less than a')

$t' = t + \rho_b = 0.19 + 0.25 = 0.44$ in. (See fig. 7.)

84. From figure 10f, the angle of the face grain with the side b is now -45° instead of 45°. The only effect of this is to change the sign of X, Y, D_5, and D_6' in equation (4) or (4_{45°) (par. 24). The changes specified in equation (13) (par. 48) must also be made. From equations (4) and (13) it is seen that

$$\left(1 + \frac{683000}{342000 \times 0.19 \times 12}\right) S_b = 1.87\, S_b$$ is substituted for S_b, and

$$N = 1.32 + \frac{4 \times 683000}{1400000 \times 0.19 \times 12} = 1.32 + 0.87 = 2.09$$

$$D_2 = 0.273 + \left(1 + \frac{(0.53/0.25)^2}{1 + \frac{683000\, n}{342000 \times 0.19 \times 10.9}}\right) \frac{\pi^2\, 683000 \times 0.25^2}{1400000 \times 0.19^3 \times 12}$$

$$= 0.273 + \left(1 + \frac{4.4}{1 + 0.97\, n}\right) 3.7 = 12.5,\ 9.7 \text{ for } n = 1,\ 2 \ldots$$

$$D_4 = 1.23 + \frac{\pi^2\, 1710}{1400000 \times 0.19^3 \times 12} = 1.23 + 0.15 = 1.38$$

$M = 1.32$; $P = 0.93$; $Q = 1.03$; $X = Y = 0$

$D_1 = D_3 = 0.273$; $D_5 = D_6 = -0.178$ (equation [4], par. 63)

The large increase in D_2 is to be expected, as this represents the greatly increased average bending stiffness in the direction of the stiffener.

From equations (5) (par. 25)

$$A_1 = 1.32 \times 1.03^2 = 1.40;\ A_2 = 0.93^2 \times 1.03 = 0.89$$

$$A_3 = (1.32 \times 2.09 - 0.93^2)\, 1.03 = 1.95 \qquad [5]$$

$C_1 = 1.36$; $C_2 = 3.83$ as before; $C_3 = 2.09 \times 1.03 = 2.15$

$$C_4 = 1.32 \times 2.09 - 0.93^2 - 2 \times 0.93 \times 1.03 \approx 0$$

From equation (15a) (par. 53) and the above values

$$\Delta_a = \frac{\pi^2 \; 57600 \times 14}{D_2 \; 1400000 \times 0.19^3 \; n \; a^2} = \frac{830}{n \; a^2 \; D_2} \qquad [15]$$

85. With the foregoing values, table III can readily be filled in, in the same way as table I. The results are plotted to determine the minimum theoretical stresses in figure 12 in the same way as figure 11. Finally, the correction factors K_1 and K_2 are calculated, and the results for both buckling between and across stiffeners are summarized in table IV, and by the dotted lines in figure 12.

Structures Department,
Chance Vought Aircraft,
Stratford, Conn.

APPENDIX

DEVELOPMENT OF THEORY

86. The theory of curved shells is much more complex than that of flat sheets and many minor quantities must be neglected to make it usable. The quantities considered in this theory are the same as are used in reference 5, in studying the torsional stability of isotropic cylinders.

87. Figure 13a shows the notation used for case A. Axes x_a and x_b are in the middle surface of the sheet in the direction of sides a and b. Axes x_α and x_β are also in the middle surface and in the direction of the face grain and the perpendicular direction, respectively (or in the direction of the principal elastic axes of the sheet). The displacement of any point in the middle surface in these directions is designated by u, with corresponding subscripts, and the displacement normal to the sheet (radially outward) by w.

88. Quantities ϵ_α, ϵ_β, and $\epsilon_{\alpha\beta}$ are the direct and shearing unit strains, and κ_α, κ_β, $\kappa_{\alpha\beta}$ the curvatures and angle of twist in the α and β directions, while f_α, f_β, $f_{\alpha\beta}$ and m_α, m_β, $m_{\alpha\beta}$ are to represent corresponding internal forces and moments per unit length of section in the face plies of a plywood sheet (fig. 2). Other notation is as used before. (See Notation at beginning of this report.)

89. Then, from Hooke's law, (assuming rotary cut plies)

$$\epsilon_\alpha = \frac{1}{(1-t_1)t}\left(\frac{f_\alpha}{E_L} - \mu_{TL}\frac{f_\beta}{E_T}\right); \quad \epsilon_\beta = \frac{1}{(1-t_1)t}\left(\frac{f_\beta}{E_T} - \mu_{LT}\frac{f_\alpha}{E_L}\right);$$

$$\epsilon_{\alpha\beta} = \frac{f_{\alpha\beta}}{(1-t_1)t\ G_{LT}} \qquad (18)$$

Similarly, using elementary plate theory

$$\kappa_\alpha = \frac{12}{(1-t_1^3)t^3}\left(\frac{m_\alpha}{E_L} - \mu_{TL}\frac{m_\beta}{E_T}\right); \quad \kappa_\beta = \frac{12}{(1-t_1^3)t^3}\left(\frac{m_\beta}{E_T} - \mu_{LT}\frac{m_\alpha}{E_L}\right);$$

$$\kappa_{\alpha\beta} = \frac{6m_{\alpha\beta}}{(1-t_1^3)t^3 G_{LT}} \tag{18'}$$

From the reciprocal theorem and experiments, it can be assumed that

$$\mu_{LT}E_T = \mu_{TL}E_L, \quad \text{or} \quad \mu_{LT} = \mu_{TL}E_L/E_T = \mu/e \tag{19}$$

From plate theory the internal strain energy in the face plies is

$$V_{\text{face plies}} = \frac{1}{2}\int\int\Big(f_\alpha\epsilon_\alpha + f_\beta\epsilon_\beta + f_{\alpha\beta}\epsilon_{\alpha\beta} + m_\alpha\kappa_\alpha + m_\beta\kappa_\beta + 2m_{\alpha\beta}\kappa_{\alpha\beta}\Big)\,dx_\alpha dx_\beta \tag{20}$$

By using equation (19) and values of $f_\alpha\ldots$, $m_\alpha\ldots$ found by solving equations (18) and (18'), in equation (20)

$$V_{\text{face plies}} = \frac{\epsilon t}{2}\int\int\left[(1-t_1)(\epsilon_\alpha^2 + e\epsilon_\beta^2 + 2\mu\epsilon_\alpha\epsilon_\beta + g\epsilon_{\alpha\beta}^2) + \frac{t^2}{12}(1-t_1^3)(\kappa_\alpha^2 + e\kappa_\beta^2 + 2\mu\kappa_\alpha\kappa_\beta + 4g\kappa_{\alpha\beta}^2)\right]dx_\alpha dx_\beta \tag{20'}$$

By making similar calculations of the strain energy in the other plies, and adding, the total internal strain energy of the sheet is found to be

$$V = \frac{\epsilon t}{2}\int\int\left[\Big(A\epsilon_\alpha^2 + B\epsilon_\beta^2 + 2\mu\epsilon_\alpha\epsilon_\beta + g\epsilon_{\alpha\beta}^2\Big) + \frac{t^2}{12}(C\kappa_\alpha^2 + D\kappa_\beta^2 + 2\mu\kappa_\alpha\kappa_\beta + 4g\kappa_{\alpha\beta}^2)\right]dx_\alpha dx_\beta \tag{21}$$

where A, B, C, D will be found to have the values given in equation (3_1) or (3_2), and so forth, (pars. 17 and 18) for the kinds and arrangements of plies described.

90. By similar reasoning it can be shown that equation (21), and subsequent equations developed from it, apply to the most general case of any kind of sheet, if $\epsilon = t = 1$; Sa, Sb..., Fa... represent forces per unit length of section instead of stresses, and

$$A = \frac{B_\alpha}{1-\mu_{\alpha\beta}\mu_{\beta\alpha}}; \quad B = \frac{B_\beta}{1-\mu_{\alpha\beta}\mu_{\beta\alpha}}; \quad \mu = \mu_{\beta\alpha}A; \quad g = B_{\alpha\beta}$$

$$C = \frac{12\,D_\alpha}{(1-\mu_{\alpha\beta}'\mu_{\beta\alpha}')t^2}; \quad D = \frac{12\,D_\beta}{(1-\mu_{\alpha\beta}'\mu_{\beta\alpha}')t^2}; \qquad (3_4)$$

$$\mu' = \mu_{\beta\alpha}'C; \quad g' = \frac{3D_{\alpha\beta}}{t^2}$$

Quantities B_α, B_β and $B_{\alpha\beta}$ are the extensional stiffnesses of the sheet in its principal elastic directions, and the shear stiffness (the forces per unit length of section required to produce unit strains); $\mu_{\alpha\beta}$ and $\mu_{\beta\alpha}$ are, respectively, the ratio of the strain in the β direction to strain in the α direction under a force in the α direction, and vice versa. Similarly, D_α, D_β, and $D_{\alpha\beta}$ are the bending stiffnesses of typical narrow strips of the sheet in the principal directions, and the torsional stiffness of a wide section of the sheet (moments per unit length of section required to produce unit curvature or twist); $\mu_{\alpha\beta}'$ and $\mu_{\beta\alpha}'$ are the ratio of the curvature in the β direction to the curvature in the α direction produced by a moment in the α direction and vice versa; μ' and g' are to be used instead of μ and g in the second line of equation (21), and $H' = 2\mu' + 4g'$ instead of $H = 2\mu + 4g$ for calculating $D_1 \ldots D_8$ in equation (4).

91. Before expression (21) can be integrated or combined with other energies, the extensional and flexural strains

must be converted to strains in the direction of the panel sides a and b. From figure 13b, the following relation obviously exists between the coordinates and the displacements in the a,b and in the α,β directions:

$$x_a = x_\alpha \sin\theta - x_\beta \cos\theta;\quad x_b = x_\alpha \cos\theta + x_\beta \sin\theta$$

$$u_a = u_\alpha \sin\theta - u_\beta \cos\theta;\quad u_b = u_\alpha \cos\theta + u_\beta \sin\theta \tag{22}$$

°2. Differentiating these equations with respect to x_α and x_β

$$\frac{\partial x_a}{\partial x_\alpha} = \sin\theta;\quad \frac{\partial x_b}{\partial x_\alpha} = \cos\theta;\quad \frac{\partial x_a}{\partial x_\beta} = -\cos\theta;\quad \frac{\partial x_b}{\partial x_\beta} = \sin\theta \tag{23}$$

$$\frac{\partial u_a}{\partial x_\alpha} = \frac{\partial u_\alpha}{\partial x_\alpha}\sin\theta - \frac{\partial u_\beta}{\partial x_\alpha}\cos\theta;\quad \frac{\partial u_b}{\partial x_\alpha} = \frac{\partial u_\alpha}{\partial x_\alpha}\cos\theta + \frac{\partial u_\beta}{\partial x_\alpha}\sin\theta$$

$$\frac{\partial u_a}{\partial x_\beta} = \frac{\partial u_\alpha}{\partial x_\beta}\sin\theta - \frac{\partial u_\beta}{\partial x_\beta}\cos\theta;\quad \frac{\partial u_b}{\partial x_\beta} = \frac{\partial u_\alpha}{\partial x_\beta}\cos\theta + \frac{\partial u_\beta}{\partial x_\beta}\sin\theta \tag{24}$$

From the theory of partial derivatives

$$\frac{\partial u_a}{\partial x_\alpha} = \frac{\partial u_a}{\partial x_a}\frac{\partial x_a}{\partial x_\alpha} + \frac{\partial u_a}{\partial x_b}\frac{\partial x_b}{\partial x_\alpha};\quad \frac{\partial u_b}{\partial x_\alpha} = \frac{\partial u_b}{\partial x_a}\frac{\partial x_a}{\partial x_\alpha} + \frac{\partial u_b}{\partial x_b}\frac{\partial x_b}{\partial x_\alpha}$$

$$\frac{\partial u_a}{\partial x_\beta} = \frac{\partial u_a}{\partial x_a}\frac{\partial x_a}{\partial x_\beta} + \frac{\partial u_a}{\partial x_b}\frac{\partial x_b}{\partial x_\beta};\quad \frac{\partial u_b}{\partial x_\beta} = \frac{\partial u_b}{\partial x_a}\frac{\partial x_a}{\partial x_\beta} + \frac{\partial u_b}{\partial x_b}\frac{\partial x_b}{\partial x_\beta} \tag{25}$$

Substituting values of $\partial x_a/\partial x_\alpha\ldots$ and $\partial u_a/\partial x_\alpha\ldots$ from equations (23) and (24) into equation (25) and solving the resulting four equations for $\partial u_\alpha/\partial x_\alpha$, $\partial u_\beta/\partial x_\beta$ and $(\partial u_\alpha/\partial x_\beta + \partial u_\beta/\partial x_\alpha)$ it is found that

$$\frac{\partial u_\alpha}{\partial x_\alpha} = \frac{\partial u_a}{\partial x_a} \sin^2\theta + \frac{\partial u_b}{\partial x_b} \cos^2\theta + \left(\frac{\partial u_a}{\partial x_b} + \frac{\partial u_b}{\partial x_a}\right) \sin\theta \cos\theta$$

$$\frac{\partial u_\beta}{\partial x_\beta} = \frac{\partial u_b}{\partial x_b} \sin^2\theta + \frac{\partial u_a}{\partial x_a} \cos^2\theta - \left(\frac{\partial u_a}{\partial x_b} + \frac{\partial u_b}{\partial x_a}\right) \sin\theta \cos\theta \quad (26)$$

$$\left(\frac{\partial u_\alpha}{\partial x_\beta} + \frac{\partial u_\beta}{\partial x_\alpha}\right) = \left(\frac{\partial u_a}{\partial x_b} + \frac{\partial u_b}{\partial x_a}\right)(\sin^2\theta - \cos^2\theta) + 2\left(\frac{\partial u_b}{\partial x_b} - \frac{\partial u_a}{\partial x_a}\right) \sin\theta \cos\theta$$

93. The curvature of the sheet in the α and β directions is, from the theory of conic sections

$$\frac{1}{r_\alpha} = \frac{\sin^2\theta}{r}; \quad \frac{1}{r_\beta} = \frac{\cos^2\theta}{r} \quad (27)$$

Then from the theory of shells and using equation (27), the extensional and shear strains in the a, b and α, β directions, in terms of the displacements, are

$$\epsilon_a = \frac{\partial u_a}{\partial x_a} + \frac{w}{r}; \quad \epsilon_b = \frac{\partial u_b}{\partial x_b}; \quad \epsilon_{ab} = \left(\frac{\partial u_a}{\partial x_b} - \frac{\partial u_b}{\partial x_a}\right) \quad (28)$$

$$\epsilon_\alpha = \frac{\partial u_\alpha}{\partial x_\alpha} + \frac{w}{r_\alpha} = \frac{\partial u_\alpha}{\partial x_\alpha} + \frac{w}{r} \sin\theta$$

$$\epsilon_\beta = \frac{\partial u_\beta}{\partial x_\beta} + \frac{w}{r_\beta} = \frac{\partial u_\beta}{\partial x_\beta} + \frac{w}{r} \cos\theta \quad (29)$$

$$\epsilon_{\alpha\beta} = \left(\frac{\partial u_\alpha}{\partial x_\beta} + \frac{\partial u_\beta}{\partial x_\alpha}\right) - 2\frac{w}{r} \sin\theta \cos\theta$$

The last term in the expression for $\epsilon_{\alpha\beta}$ comes from the fact that the dimension d_a of an element such as in figure 13c undergoes a unit strain w/r, while the dimension d_b is unaffected by w and the curvature. Hence, unless $\theta = 0^\circ$ or 90° the two diagonals undergo

different strains owing to the curvature; this can easily be shown to result in the shear strain given.

94. Substituting values of $\partial u_a/\partial x_a$... and $\partial u_\alpha/\partial x_\alpha$... from equations (28) and (29) into equation (26) the relation between extensional strains in the a,b and α,β directions is obtained:

$$\epsilon_\alpha = \epsilon_a \sin^2\theta + \epsilon_b \cos^2\theta + \epsilon_{ab} \sin\theta\cos\theta$$

$$\epsilon_\beta = \epsilon_b \sin^2\theta + \epsilon_a \cos^2\theta - \epsilon_{ab} \sin\theta\cos\theta \qquad (30)$$

$$\epsilon_{\alpha\beta} = \epsilon_{ab}(\sin^2\theta - \cos^2\theta) + 2(\epsilon_b - \epsilon_a)\sin\theta\cos\theta$$

95. To obtain a similar relation for the flexural strains, the theory of partial derivatives gives the relations

$$\frac{\partial^2 w}{\partial x_\alpha^2} = \frac{\partial^2 w}{\partial x_a^2}\left(\frac{\partial x_a}{\partial x_\alpha}\right)^2 + \frac{\partial^2 w}{\partial x_b^2}\left(\frac{\partial x_b}{\partial x_\alpha}\right)^2 + 2\frac{\partial^2 w}{\partial x_a \partial x_b}\frac{\partial x_a}{\partial x_\alpha}\frac{\partial x_b}{\partial x_\alpha}$$

$$\frac{\partial^2 w}{\partial x_\beta^2} = \frac{\partial^2 w}{\partial x_a^2}\left(\frac{\partial x_a}{\partial x_\beta}\right)^2 + \frac{\partial^2 w}{\partial x_b^2}\left(\frac{\partial x_b}{\partial x_\beta}\right)^2 + 2\frac{\partial^2 w}{\partial x_a \partial x_b}\frac{\partial x_a}{\partial x_\beta}\frac{\partial x_b}{\partial x_\beta} \qquad (31)$$

$$\frac{\partial^2 w}{\partial x_\alpha \partial x_\beta} = \frac{\partial^2 w}{\partial x_a^2}\frac{\partial x_a}{\partial x_\alpha}\frac{\partial x_a}{\partial x_\beta} + \frac{\partial^2 w}{\partial x_b^2}\frac{\partial x_b}{\partial x_\alpha}\frac{\partial x_b}{\partial x_\beta} + \frac{\partial^2 w}{\partial x_a \partial x_b}\left(\frac{\partial x_b}{\partial x_\alpha}\frac{\partial x_a}{\partial x_\beta} + \frac{\partial x_a}{\partial x_\alpha}\frac{\partial x_b}{\partial x_\beta}\right)$$

From shell theory the curvature and unit twists in the a,b and α,β directions are

$$\kappa_a = \frac{\partial^2 w}{\partial x_a^2}; \quad \kappa_b = \frac{\partial^2 w}{\partial x_b^2}; \quad \kappa_{ab} = \frac{\partial^2 w}{\partial x_a \partial x_b} \qquad (32)$$

$$\kappa_\alpha = \frac{\partial^2 w}{\partial x_\alpha^2}; \quad \kappa_\beta = \frac{\partial^2 w}{\partial x_\beta^2}; \quad \kappa_{\alpha\beta} = \frac{\partial^2 w}{\partial x_\alpha \partial x_\beta} \qquad (33)$$

By use of these expressions for $\partial^2 w/\partial x_a^2 \ldots$ and equation (23) in equation (31) the relations between the flexural strains in the a,b and α,β directions are obtained.

$$\kappa_\alpha = \kappa_a \sin^2\theta + \kappa_b \cos^2\theta + 2\kappa_{ab} \sin\theta \cos\theta$$

$$\kappa_\beta = \kappa_b \sin^2\theta + \kappa_a \cos^2\theta - 2\kappa_{ab} \sin\theta \cos\theta \qquad (34)$$

$$\kappa_{\alpha\beta} = \kappa_{ab}(\sin^2\theta - \cos^2\theta) + (\kappa_b - \kappa_a)\sin\theta\cos\theta$$

96. Now substituting equations (30) and (34) into the strain energy expression (21), the following is obtained

$$V = \frac{\epsilon t}{2}\iint\left\{1/4\left[M\epsilon_a^2 + N\epsilon_b^2 + 2P\epsilon_a\epsilon_b + Q\epsilon_{ab}^2 + 2X\epsilon_b\epsilon_{ab} + 2Y\epsilon_a\epsilon_{ab}\right] + \frac{t^2}{\pi^2}\left[D_1\kappa_a^2 + D_2\kappa_b^2 + D_7\kappa_a\kappa_b + (D_4 - D_7)\kappa_{ab}^2 + 2D_5\kappa_b\kappa_{ab} + 2D_6\kappa_a\kappa_{ab}\right]\right\} dx_a dx_b \qquad (35)$$

where $M, N \ldots, D_1, D_2 \ldots$ have the values given in equation (4) (par. 24) and D_7 is a similar expression which cancels out later. Since only a uniform rotation of axes is involved the elemental area $dx_a dx_b$ can be substituted directly for $dx_\alpha dx_\beta$.

97. From shell theory the external loads, represented by the stresses S_a, S_b, and S_s on the edges of the sheet, do the work

$$T = \frac{t}{2}\iint\left[S_a\left(\frac{\partial w}{\partial x_a}\right)^2 + S_b\left(\frac{\partial w}{\partial x_b}\right)^2 + 2S_s\frac{\partial w}{\partial x_a}\frac{\partial w}{\partial x_b}\right]dx_a dx_b \qquad (36)$$

The work done by the pressure $S_a t/r$ (fig. 3a), if this is present (there would be such a pressure in an application such as a submarine hull, for example), will practically cancel if there are many waves in a panel, or many connected panels as in semimonocoque construction; it is the accompanying tangential compression, S_a which is important for buckling.

98. In studying the case of buckling <u>across stiffeners</u> it is assumed for simplicity that their effect is the same as if their bending, extensional, and torsional stiffness were uniformly distributed over the sheet. It can be shown that, for the sinusoidal deformation assumed, this gives no error when the slope of the waves, γ is zero, and only a small error for the angles involved in ordinary problems. Consider first the case of stiffeners running in the a direction. The extra strain energy of extension, bending and torsion owing to the presence of the stiffeners is

$$V' = \frac{1}{2}\int\int\left(\frac{E_a'A_a'}{b'}\epsilon_a^2 + \frac{E_a'I_a'}{b'}K_a^2 + \frac{G_a'J_a'}{b'}K_{ab}^2\right)dx_a dx_b \quad (37)$$

where I_a' is the moment of inertia, about their combined center of gravity, of the stiffener and effective width of sheet acting with it in bending, minus the moment of inertia of the effective width alone. The energy associated with the latter has already been considered in equation (35), and by omitting it here, equation (37) represents only energy additional to equation (35)

99. In figure 14, taking moments about the center of gravity of the combination

$$E_a'A_a'\,\delta = E_a\,t\,w_a\,(h_a - \delta) \quad (38)$$

then

$$E_a'I_a' = E_a\,t\,w_a\,(h_a - \delta)^2 + E_a'A_a'\,(\delta^2 + \rho_a^2) \quad (39)$$

Eliminating δ between equations (38) and (39)

$$E_a'I_a' = \left(1 + \frac{h_a^2/\rho_a^2}{1 + \frac{E_a'A_a'}{E_a\ t\ w_a}}\right) E_a'A_a'\rho_a^2 \qquad (40)$$

100. If the flange of the T-beam of figure 14 were infinitely wide, and all materials isotropic, with Poisson's ratio = 0.3, then from Karman's theory of the effective width of wide flanged beams (reference 4, vol. II, p. 57)

$$w_a \left[= 2\ \lambda_x = 0.363\ l\right] = 0.363\ \frac{a}{m} \qquad (41)$$

where $[l] = a/m$ is the half wave length of the bending deformation.

101. However, this effective width increases almost directly as the relative shear stiffness and inversely as the relative extensional stiffness of the flange (the sheet in our case). Hence, in this case the effective width should be

$$w_a = 0.363\ \frac{a}{m}\ \frac{2(1 + 0.3)G_{ab}}{E_a} \approx \frac{a}{m}\ \frac{G_{ab}}{E_a} \qquad (42)$$

where G_{ab} is the shear modulus of the sheet in the a and b directions, and the factor $2(1 + 0.3)$ represents the ratio E_a/G_{ab} for the isotropic material assumed in equation (41). The stiffness of the rib (the stiffener in this case) does not enter these relations — as far as this action is concerned the rib acts merely as a means of applying extensional strains along the middle of the sheet. From the derivation of equation (35) it can be seen that $Q\epsilon/4 = G_{ab}$, while $M\epsilon/4 = E_a/(1 - \mu^2/e) > E_a$. It is therefore conservative to use

$$w_a = \frac{a}{m}\ \frac{Q\epsilon/4}{M\epsilon/4} = \frac{aQ}{mM} \qquad (43)$$

The rule of equation (12') follows from this and the obvious fact that the effective width should not be taken to exceed the distance between stiffeners b'.

102. During buckling across stiffeners there will be an additional external work owing to the stress S_a' on the stiffeners, of

$$T' = 1/2 \int\int S_a' \frac{A_a'}{b'} \left(\frac{\partial w}{\partial x_a}\right)^2 dx_a dx_b$$

$$= 1/2 \int\int S_a \frac{E_a'}{E_a} \frac{A_a'}{b'} \left(\frac{\partial w}{\partial x_a}\right)^2 dx_a dx_b \quad (44)$$

103. If the energies expressed by equations (37), (40), (43), and (44) are added to those of (35) and (36), this is obviously equivalent to making the changes in S_a, M, D_1, and D_4 specified in equations (12) and (12') (pars. 42 and 45). The changes specified in equations (13) and (13'), for the case of buckling across stiffeners running in the b direction, can be derived in a similar manner.

104. If the shape of the deformation were known, the condition for buckling would be simply that the work done by external forces, owing to the deformation, is equal to the change in internal energy, or $T = V$. Since the shape is not known, various shapes similar to those observed in experiments must be tried by the energy method and the one must be selected which minimizes either the total energy change $T - V$ or the buckling load (reference 6, p. 144). The displacement normal to the sheet will be assumed to be

$$w = W \sin \frac{m\pi(x_a + \gamma x_b)}{a} \sin \frac{n\pi x_b}{b} \quad (45)$$

where m, n and γ are chosen to minimize the buckling load. This expression describes a wave form with half wave lengths a/m and b/n in the a and b directions, and with nodes parallel to the a direction and at a slope γ to the b direction (fig. 3a). This

permits a close approximation to the shapes found experimentally in all the cases covered by the theory.

105. As to boundary conditions for w, it will be assumed that the nodes of the deformation always coincide as closely as possible with some stiffener, that is, that the deformation will be as in figure 15a for buckling between stiffeners, and as in figure 15b for buckling across stiffeners. According to equation (45) the nodes cannot lie exactly along stiffeners in the b direction, but it is assumed that they do this as nearly as possible, straddling the stiffener as shown in figures 8a and 16. All this requires that m and n be whole numbers, or that a and b be whole multiples of a' and b'.

THE CORRECTION FACTOR λ

106. For the case of buckling of the panel between stiffeners, of course, the node actually does lie all along the side b, and a correction factor $1/\lambda$ is applied to the buckling stress to allow for the fact that the deformation is not exactly as described by equation (45). Several things about this factor can be told from general reasoning. It must equal unity when the slope $\gamma = 0$. In general it must be greater than one (or λ must be less than one) when γ is different from zero. This can be appreciated by imagining first that the stiffeners along sides b are removed; the buckling stress obtained by using equation (45) would be about correct for this physical case. If, now, stiffeners are attached along these positions and their stiffness is increased until all lateral displacements along these positions are prevented, the resistance to buckling is obviously increased.

107. This increase will evidently be larger, the larger the slope γ. Also it seems obvious that there will be more increase in a case such as shown at (b), figure 16, and less increase for a case such as shown at (c) than for the case shown at (a) although γ is the same for all these cases. There is no reason to expect cases (d) or (e) to require a much different correction from case (a); however, it is reasonable to believe that a case such as shown at (f) would require little correction compared to case (a), since much less readjustment in the position of nodes would be necessitated. All these and other

"common sense" reasonings are satisfied if it is assumed that $1/\lambda$ or λ is some function of the ratio to the total area, of the area which would have to be swept through in moving nodes from the positions described by equation (45) to their true positions (or the areas shown shaded in fig. 16).

108. For the cases such as figure 16a, b,... and e this ratio is

$$(4 \times 1/2 \times b/2 \times b/2\ \gamma)/(ab) = \frac{b\gamma}{2a}$$

and λ could be therefore taken as a function of $b\gamma/a$. It will be found that the reduction in "adjustment area" which is possible in special cases, such as figure 16f, is very nearly compensated for by dividing this by a factor n', plotted in figure 5a.

109. The values of λ in the left half of figure 5b were obtained by comparing the present theory with known correct values for the buckling of an isotropic flat panel under shear. Near the middle of figure 5b, where the correction amounts to a good deal, the curve was drawn somewhat higher (that is, on the conservative side) than this comparison indicated, because of the uncertainty involved in using such results for other cases. For small values of $b\gamma/an'$ the boundary condition correction just discussed is unimportant, and the opposite tendency of energy method solutions to give too high a value for the buckling load becomes dominant, so that $1/\lambda$ rises a little above unity. It comes back to unity when γ and $b\gamma/an'$ are zero, because the shape given by equation (45) then becomes the exact solution.

110. Figure 17 shows a comparison between results obtained by using figure 5b with the present theory, and the best known values for this case. It will be seen that the present theory is probably about right for large values of a/b, which involve use of the leftmost part of figure 5b, and is quite conservative for small values of a/b, involving the use of points near the middle of figure 5b.

111. The right hand side of figure 5b was conservatively extrapolated from the already conservative left side, remembering also that $1/\lambda$ should not become negative; it

was included for completeness, but it is not needed for most practical problems, as the critical conditions will be found to lie in the left side of this figure. This correction factor is admittedly very rough; but as indicated it only amounts to as much as 30 percent or so in a few applications, and there is little doubt that at least that much is justified for such cases.

112. We must now complete our expressions for the displacement. As previously discussed, in the case of curved shells, displacements in the plane of the sheet must be considered as well as in the normal direction. These will be assumed to be

$$u_a = U_a \frac{b}{\pi n r} \cos \frac{m\pi(x_a + \gamma x_b)}{a} \sin \frac{n\pi x_b}{b}$$

$$u_b = U_b \frac{b}{\pi n r} \sin \frac{m\pi(x_a + \gamma x_b)}{a} \cos \frac{n\pi x_b}{b} \qquad (46)$$

where the quantities U_a and U_b, describing the magnitudes of these displacements, will be determined by minimizing the energy. These expressions bear the same general relation to the expression for normal displacement (equation (45)) as the corresponding expressions found in exact solutions of shell problems, and since they permit a large reduction in the energy they must be close to the correct value. The boundary conditions for u_a and u_b specified in the first part of this report (par. 12) are automatically satisfied by using equation (46).

113. Equations (45) and (46) can now be substituted into the expressions (28) and (32) for ϵ_a..., κ_a... and the resulting quantities can be substituted into the expression for total energy change during the buckling displacement. Using the correction factor λ, this energy change can now be taken as $T - V/\lambda$, where T and V are given by equations (35) and (36). By making these substitutions, carrying out the integrations and simplifying, the total energy change is found equal to certain constant factors times

$$W^2\left[\beta^2 S_a + (1+\beta^2\gamma^2)S_b + 2\beta^2\gamma S_s\right] = \frac{m^2 S}{\lambda}\left\{\left[M(\beta U_a - W)^2\right.\right.$$

$$+ NU_b^2(1+\beta^2\gamma^2) + 2PU_b(\beta U_a - W) + QU_b\beta(\beta U_b + 2U_a)$$

$$\left.\left. + QU_a^2(1+\beta^2\gamma^2) + 2XU_b\beta\gamma(\beta U_b + 2U_a) + 2YU_a\beta\gamma(\beta U_a - W)\right]\left(\frac{\alpha}{mn}\right)^2\right.$$

$$+ W^2\left[D_1\beta^2 + D_2(1+\beta^2\gamma^2)^2/\beta^2 + D_3 4\gamma^2 + D_4(1+\beta^2\gamma^2)\right.$$

$$\left.\left. + D_5(2\beta^2\gamma^3 + 6\gamma) + D_6 2\beta^2\gamma\right]\right\} \qquad (47)$$

114. Setting the derivatives of expression (47) with respect to W, U_a and U_b equal to zero, eliminating U_a and U_b between the resulting three equations and simplifying, results in the following expression (except for the term $0.03\beta^4 C_1$, which has been added for reasons discussed later)

$$\beta^2 S_a + (1+\beta^2\gamma^2)S_b + 2\beta^2\gamma S_s = S\frac{m^2}{\lambda}$$

$$\left[\frac{A_1\beta^2\gamma^2 + A_2(1+\beta^2\gamma^2)\gamma^2 + A_3(1+\beta^2\gamma^2)^2/\beta^2 + A_4 2\beta^2\gamma^3 + A_5 4\gamma^3 + A_6 2\gamma}{C_1(\beta^2+0.03\beta^4) + C_2\beta^2\gamma^2 + C_3(1+\beta^2\gamma^2)^2/\beta^2 + C_4(1+\beta^2\gamma^2) + C_5 2\beta^2\gamma^3 + C_6 4\gamma^2 + C_7 2\gamma + C_8 2\beta^2\gamma}\right.$$

$$\times\left(\frac{\alpha}{mn}\right)^2 + D_1\beta^2 + D_2(1+\beta^2\gamma^2)^2/\beta^2 + D_3 4\gamma^2 + D_4(1+\beta^2\gamma^2)$$

$$\left. + D_5(2\beta^2\gamma^3 + 6\gamma) + D_6 2\beta^2\gamma\right] \qquad (7a')$$

where $A_1 \ldots A_6$, $C_1 \ldots C_7$ have the values given in equation (5)(par. 25). This is the same equation as (7a) (par. 30) and the values of $s_{a..}$, $A_1 \ldots$, $c_1 \ldots$, $d_1 \ldots$ (which are charted in fig. 9) are as indicated in equation (7a'). The added term $0.03\beta^4 C_1$ has a negligible effect in ordinary problems,

but has been arbitrarily added because it was found to greatly improve the accuracy in such extreme applications as the torsion of long tubes. It obviously has a conservative effect in any case.

115. Case B. This case is developed in a manner similar to case A and the result is the same as given in equation (7a') except that the numerator of the long fraction is replaced by

$$B_1\beta^2 + B_2\beta^2\gamma^2 + B_3(1 + \beta^2\gamma^2)\gamma^2 + B_4 2\beta^2\gamma^2 + B_5 2\beta^2\gamma \quad (7b')$$

where $B_1 \ldots B_5$ also have the values given in equation (5). This then coincides with equation (7b)(par. 40) and the values of $b_1 \ldots b_5$ are as indicated.

THE CORRECTION FACTORS K_1 AND K_2

116. Figure 6, used for determining K_1, needs little explanation. It may be considered as representing the relations between the Euler formula and the usual rules for designing columns in the long and short ranges, generalized so as to be applicable to any type of stability problem. Using the broken line marked "ideal" is equivalent to using the stress at which buckling would theoretically occur, or the stress at which yielding of the material would occur, whichever is the smaller. The horizontal part of the line corresponds to the range in which buckling occurs first, and the sloping to the range in which the material yields first.

117. The other lines allow for the fact that partial failure of the material between the proportional limit and the yield point (which can be considered for the present purpose to coincide with the "compressive strength" for wood), as well as initial crookedness and other equivalent imperfections, all reduce the ideal strength, especially when the structure is near to both types of failure. The curve marked "good construction" follows closely the short column formula given in reference 1 (p. 59) except for more allowance for the effect of imperfections in the long column range. The curve marked "rough construction" is close to some of the more pessimistic column formulas. Most reliable strut tests fall between the two curves.

118. Figure 7, used for obtaining K_3, is an attempt to consider the fact that tests on metal cylinders, especially under axial compression, have always shown large deviations from theory. This is true even when the buckling stresses are far below the proportional limit of the material, so that the cylinders are far into the "long column" range, and the factors considered in figure 6 afford no explanation. The experimental strength varies from nearly 100 percent down to 20 percent and less, of the theoretical, so that blanket reduction factors are hardly practical. To devise a reasonable way to allow for such discrepancies under any and all conditions requires some understanding of the causes of the phenomenon.

119. This question has long been controversial but a reasonable explanation has recently been made possible by researches of Kármán and Tsien (reference 7) although the explanation suggested by these authors does not in itself seem very satisfactory. If the load on a "porfect" strut is plotted against its lateral deflection, as shown in figure 18a, a horizontal or slightly rising line after buckling is obtained. Practical struts with initial defects give curves which approach this horizontal line more or less rapidly, depending on the amount of initial curvature or other defect. Yielding eventually occurs owing to the combination of direct and bending stress, and the curve breaks downward, the load at this point measuring about the maximum resistance. This maximum resistance, for struts which are not close to yielding when they buckle, is obviously not much less than that of the perfect strut, and depends but little on the magnitude of the initial defects.

120. On the other hand, Kármán and Tsien (using a large deflection theory which it would be impractical to apply to our general problem) have shown that a compressed perfect cylinder behaves, as shown in figure 18b, offering the same resistance at first as is indicated by conventional theories such as the present one, but with rapidly falling resistance as the deflection increases. Comparison of figures 18a and 18b makes it evident that a practical cylinder with initial defects must behave as is indicated, and will have a maximum resistance which is <u>much less</u> than that of the perfect cylinder and which is <u>very dependent</u> on the magnitude of the initial defects, even when no yielding of the material occurs.

121. This conclusion that the reduction in strength depends principally on the initial imperfections in shape, suggests

first that the reduction should be a function of the radius thickness ratio r/t, as it is well known that such defects are relatively much greater in very thin cylinders (reference 5, p. 7). It is also logical that the reduction should be a function of the total number of buckles over the surface of the specimen mn because the chance of large imperfections of an unfavorable shape being present over an area corresponding to some of the buckles obviously increases with the total number of buckles which may occur.

122. Figure 19 shows the rather remarkable coordination of all the available test results on cylinders which it has been found possible to achieve on this basis. The vertical coordinates of the points represent the ratio between the experimental strength and the strength as given by the present theory, while the horizontal coordinates are calculated from the critical m and n predicted by the theory. There is still a good deal of scatter, but there obviously must be much scatter in the occurance of unfavorable defects in shape, and the scatter is less than has ever before been obtained in attempts to coordinate such test results.

123. The two curves in figures 7 and 19 represent the minimum and near-minimum of the points. If an allowance for scatter is made in selecting the modulus of elasticity of the material, as discussed in paragraph 16, and if it is considered that a good many of the uncertainties which general factors of safety ordinarily have to cover are being separately allowed for, it seems conservative to use the good construction curves of both figures 6 and 7 for the design of aircraft structures.

CONSIDERATION OF EDGE FIXITIES

124. The method presented (par. 53) is a rough approximation, which is advanced as being quite practical to use, and, since it gives reasonable results even in extreme cases, as being greatly preferable to the common practice of neglecting edge fixities or guessing at their effects. It makes the assumption that the effect of fixity along, say, the edges a can be approximated by a suitable modification of the bending stiffness in the direction perpendicular to these edges. This assumption seems basically logical if it is considered, for instance, that such edge

fixity would have no effect whatever if this bending stiffness happened to be zero, no matter what the other stiffnesses were.

125. The method was derived by experimenting with various functions which general experience indicated to be reasonable, or which were suggested by approximate solutions of simplified cases, and has been checked by comparing it to various special known solutions. Since its justification depends entirely on these checks, and since they should cover the hinged as well as other edge conditions, they are discussed all together in the following section.

CHECKS WITH PREVIOUS THEORIES

126. First compare results obtained from this theory (without the factors K_1 or K_2) with previous theories, in the ranges for which the latter apply. Most previous theories for anisotropic plates or shells neglect Poisson's ratio effects and make other assumptions whose general validity is uncertain. Hence, the only anisotropic theory for which a comparison will be made is that of reference 2, which gives the stability conditions for flat hinged-edged plywood panels under combinations of shear and compression in one direction. It is reassuring that the present theory, although derived independently, coincides exactly with this theory for this case when the panels are of infinite length. The following table of equivalent notations is given for convenience in comparing the two theories. The previous theory is an approximate energy solution similar to the present one, but its method of taking care of the anisotropic elastic properties of the sheet is entirely rational; this is, therefore, an excellent check on this phase of the present theory.

Reference 2	a	b	h	z	θ	γ	p_{cr}	q_{cr}	E_1	E_2	A
Present theory	b	a/m	t	$1/\beta$ (n=1)	$-\theta$	γ	S_a	S_s	CE	DE	HE/2

127. The present theory differs from the previous one in the correction for the finite length of the panel. The present method does this by requiring the number of half waves m to be a whole number, and uses a correction

factor λ only for the interference with the angularity of the waves at the panel ends. The method of reference 2 assumes first a wave length the same as for an infinitely long panel, and corrects (for the shear stress only) for the interference with both the angularity and this length of wave, owing to the panel ends, by a factor $k_s/(k_s)_\infty$; this simplifies the method, but this simplification could not be used in the general application of the present theory in any case.

128. Further checks can be obtained with previous theories for isotropic plates and shells. For isotropic sheets, equations (4_{iso}) and (5) (par. 25) inserted in equation (7a') give for the case A and hinged edges:

$$\beta^2 S_a + (1+\beta^2\gamma^2)S_b + 2\beta^2\gamma S_s = S\frac{m^2}{\lambda}\left[\frac{\pi^2}{12}\left(\beta^2+\frac{1}{\beta^2}+6\gamma^2+\beta^2\gamma^4+2+2\beta^2\gamma^2\right)\right.$$

$$\left.+\frac{2(1-\mu)\beta^2\gamma^2+4\mu^2(1+\beta^2\gamma^2)\gamma^2+4(1-\mu^2)(1+\beta^2\gamma^2)^2/\beta^2}{\beta^2+0.03\beta^4+[(1+\mu)^2/(2-2\mu)]\beta^2\gamma^2+(1+\beta^2\gamma^2)^2/\beta^2+2(1+\beta^2\gamma^2)}\left(\frac{\alpha}{mn}\right)^2\right] \quad (7_{iso})$$

129. For the case of a cylinder in torsion $S_a = S_b = 0$; $\lambda = 1$. Selecting γ, m, and n (n always equals 1 in such a case) to minimize S_s, and assuming $\mu = 0.3$, the results in table V are obtained. If the edges at the ends of the cylinders are fixed, then from equation (15a) (par. 53) $\Delta_a = \infty$; $\Delta_2 = (n+1)^2/n^8 = 4$, and the long parenthesis in the above equation is changed to

$$\left(\beta^2+\frac{4}{\beta^2}+12\gamma^2+4\beta^2\gamma^4+2+2\beta^2\gamma^2\right) \quad (7_{iso}')$$

Again selecting γ and m to minimize S_s, results which are also shown in the table, are obtained. Table V also shows the results obtained with the previous theory (reference 5) for the same cases. For long cylinders the correction for edge fixity evidently has less effect than it should have, but the effect is not very important here.

TABLE V

b^2/rt		200		2000		20,000	
General description		Short cylinder		Medium length cylinder		Long cylinder	
Edge	Condition	Hinged	Fixed	Hinged	Fixed	Hinged	Fixed
$\frac{S_s}{E}\left(\frac{b}{t}\right)^2$	Reference 5	43	50	220	240	1300	1400
	Present theory	44	49	230	235	1320	1330

130. For the case of a cylinder under axial compression $S_a = S_s = 0$, $\lambda = 1$. The minimum S_b is obtained in this case when $\gamma = 0$ and m and n are in general both greater than one. It can easily be shown that the present theory checks the "classical" theory exactly for this case except for the term $0.03\beta^4 C_1$ ($0.03\beta^4$ in equation (γ_{iso})) which has only the slight effect here of reducing the value found for S_b by a fraction of 1 percent. There is no exact solution available to check the effect of edge fixity in this case, but the correction for edge fixity of the present theory has little effect in this case unless the cylinder is very short, which is entirely in accord with test experience.

131. Similar results are found in comparing the present theory with known theories for the buckling of curved panels under axial compression. All these cases constitute a good check of the treatment of the effect of curvature in the present theory.

132. Numerous solutions for the stability of isotropic flat panels are available for comparison. For this case $r = \infty$, $\alpha = 0$ and the condition for stability reduces to the first line alone of equation (γ_{iso}). The curves of figure 17 show the results of applying this equation to the case of shear on a hinged-edged panel, compared to known solutions. A similar check is obtained for the case of shear on an infinitely long panel with the long sides fixed. No exact solution is available, for comparison, for a finite panel with fixed edges.

133. Figure 20 shows a comparison between the present theory and the exact (reference 8, p. 168) for compressive loading of various shapes of panels, under various extreme edge conditions. The curves are extended beyond the range in which $a > b$, as such a limitation is not necessary for this case. These cases of panels under widely varying conditions of loading, edge fixity, and proportions, with maximum errors of 20 percent on the conservative side and 10 percent on the unconservative side, represent a reasonable check of the present theory's treatment of panel size and complete edge fixity.

134. The treatment of fixities intermediate between zero (hinged) and complete fixity, and owing to the torsional stiffness of the member to which the panel edge is attached, can be checked against a solution by Dunn (reference 9). Figure 21 shows how the results obtained with the present theory compare with this previous theory for the case when a is greater than b, and for various torsional stiffnesses of the side members. The case considered here is that of several adjacent and similarly loaded panels, as in semi-monocoque construction, so that the effect of each side member is divided between two panels.

135. The treatment of intermediate fixities owing to distributed elastic resistance to rotation can be checked against the case of a strut with elastically clamped ends. A very long flat panel, under compression S_b in the direction of the short side, is under the same condition as a strut, except that the "plate modulus" $\epsilon = E/(1 - \mu^2)$ takes the place of E. This is the only kind of buckling of stiffened panels which is considered in reference 1. Figure 22 shows the results obtained with the present theory for a simple isotropic panel under these conditions, compared to the exact solution. A similar check could be expected for plywood and for stiffened panels if an exact solution were available for comparison.

EXPERIMENTAL CHECKS

136. Figure 19 affords a comparison between the present theory, with the correction factors K_1 and K_2 and numerous tests on cylinders. Unfortunately tests on panels of metal or plywood have almost all been made under indeterminate edge conditions, and also practically all available

reports on tests of plywood panels or cylinders are lacking in some of the essential data. Tests on plywood constructions under determinate conditions are greatly needed. Figure 23 suggests a method of testing which would permit the conditions of the sheet to be known and to approximate those in semi-monocoque construction, and which would at the same time permit the resistance of the sheet to be isolated from that of longitudinal stiffeners.

137. The tests of plywood cylinders included in figure 19 are taken from the most complete reports available, but some of the data were uncertain even in these cases. This quite possibly accounts for the greater scatter in these tests compared to metal cylinders.

REFERENCES

1. Anon.: ANC Handbook on the Design of Wood Aircraft Structures. ANC Committee on Aircraft Design Criteria. July 1942.

2. March, H. W.: Buckling of Flat Plywood Plates in Compression, Shear, or Combined Compression and Shear. Mimeo. No. 1316, Forest Products Lab., April 1942.

3. von Kármán, Theodore, Sechler, Ernest E., and Donnell, L. H.: The Strength of Thin Plates in Compression. Trans. A.S.M.E., vol. 54, 1931, pp. 53–57.

4. Timoshenko, S.: Strength of Materials. D. Van Nostrand Co., 2d ed., 1941.

5. Donnell, L. H.: Stability of Thin-Walled Tubes under Torsion. Rep. No. 479, NACA, 1933.

6. Donnell, L. H.: I. The Problem of Elastic Stability. A.S.M.E. Trans., Aero. Div., 1933.

7. von Kármán, Theodore, and Tsien, H. S.: The Buckling of Thin Cylindrical Shells under Axial Compression. Jour. Aero. Sci., June 1941, pp. 303–312.

8. Sechler, Ernest E., and Dunn, Louis G.: Airplane Structural Analysis and Design. John Wiley and Sons, Inc., 1942.

9. Dunn, Louis G.: An Investigation of Sheet–Stiffener Panels Subjected to Compression Loads with Particular Reference to Torsionally Weak Stiffeners. T.N. No. 752, NACA, 1940.

TABLE I - Typical Tabular Solution of Case B Problem

(Use similar form for Case A problem except A_1, A_2—, a_1, a_2—A' are substituted for B_1, B_2—, b_1, b_2—B')

$\frac{m}{n}$	$\frac{1}{2}$	$\frac{1}{1}$	$\frac{2}{1}$	$\frac{3}{1}$	$\frac{4}{1}$	$\frac{\infty}{1}$
$\Delta_1 D_1 = .273\left(\frac{1+21.2\frac{(m+1)n^2/m^2s}{n^2/m}}{1+21.2\ n^2/m}\right)$ (eq.15b)	1.08	1.05	.58	.46	.40	.48
$\Delta_2 b_2 = .273\left(\frac{1+.40\frac{(n+1)n^2/n^2s}{m^2/n}}{1+.40\ m^2/n}\right)$ (eq.15a)	.32	.45	.71	.87	.95	.48
$\beta = \frac{bm}{an} = .86\frac{m}{n}$	.43	.86	1.72	2.57	3.43	1.29
τ	0 .25 .50 .75	0 .25 .50 .75	0 .25 .50 .75	0 .25 .50 .75	0 .25 .50 .75	0 .25 .50 .75
$B_1b_1 = .90\ b_1$	.17 .17 .17 .17	.67 .67 .67 .67	2.67 2.67 2.67 2.67	6.1 6.1 6.1 6.1	10.7 10.7 10.7 10.7	1.53 1.53 1.53 1.53
$B_2b_2 = 2.56\ b_2$	0 .03 .12 .26	0 .12 .49 1.05	0 .47 1.92 4.20	0 1.0 4.3 9.5	0 1.8 7.4 16.3	0 .26 1.07 2.38
$B_3b_3 = 1.79\ b_3$	0 .11 .46 1.08	0 .12 .52 1.37	0 .13 .78 2.62	0 .2 1.2 4.8	0 .2 1.8 7.6	0 .12 .62 1.93
$\Sigma B_1b_1 = "B"$	.17 .31 .75 1.51	.67 .91 1.68 3.09	2.67 3.27 5.37 9.49	6.1 7.3 11.6 20.4	10.7 12.7 19.9 34.6	1.53 1.91 3.22 5.84
$C_1c_1 + C_2c_2 = 1.36\ (c_1 + c_2)$	7.5 8.0 8.5 9.4	2.75 2.96 3.60 4.67	4.8 5.1 5.8 7.6	11.0 11.3 12.6 15.4	21.0 21.4 23.5 28.0	3.2 3.4 4.0 5.4
$C_1c_1 = 3.84\ c_1$	0 0 .2 .4	0 .17 .71 1.55	0 .7 2.8 6.4	0 1.6 6.4 14.0	0 2.7 11.3 25.0	0 .4 1.6 3.5
$C_2c_2 = -1.04\ c_2$	-1.0 -1.1 -1.1 -1.2	-1.04 -1.10 -1.26 -1.47	-1.0 -1.2 -1.8 -2.7	-1.0 -1.5 -2.7 -4.9	-1.0 -1.8 -4.0 -7.8	-1.0 -1.1 -1.5 -2.0
$\Sigma c_1c_1 = "C"$	6.5 6.9 7.6 8.6	1.71 2.03 3.06 4.75	3.8 4.6 6.8 11.3	10.0 13.4 16.3 24.5	20.0 22.3 30.8 45.2	2.2 2.7 4.1 6.9
$\left(\frac{\alpha}{an}\right)^2 = \left(\frac{4.7}{an}\right)^2 = d_0$	5.53	22.1	5.54	2.46	1.38	.61
$D_0d_0 = B'/C'\ d_0$	.14 .25 .54 .97	8.6 9.9 12.1 14.4	3.91 3.95 4.40 4.66	1.5 1.6 1.8 2.1	.7 .8 .9 1.1	.42 .45 .48 .52
$(A_1D_1)d_1$	.20 .20 .20 .20	.8 .8 .8 .8	1.72 1.72 1.72 1.72	3.1 3.1 3.1 3.1	4.8 4.8 4.8 4.8	.82 .82 .82 .82
$(A_2D_2)d_2$	1.70 1.77 1.90 2.13	.6 .7 .9 1.2	.24 .33 .73 1.72	.1 .3 .9 2.9	.1 .2 1.3 4.7	.28 .35 .59 1.07
$D_3d_3 = .273\ d_3$	0 .07 .27 .62	0 .1 .3 .6	0 .07 .27 .62	0 .1 .3 .6	0 .1 .3 .6	0 .07 .27 .62
$D_4d_4 = 1.23\ d_4$	1.23 1.24 1.32 1.38	1.2 1.3 1.5 1.7	1.23 1.43 2.10 3.10	1.2 1.7 3.2 5.8	1.2 2.1 4.8 9.2	1.23 1.34 1.73 2.33
$\sum D_1d_1 = "D"$	3.27 3.53 4.23 5.30	11.2 12.8 15.6 18.7	7.10 7.50 9.22 11.82	5.9 6.8 9.3 14.5	6.8 8.0 12.1 20.4	2.75 3.01 3.89 5.36
$(D_5d_5 + D_6d_6) = .178\ (d_5 + d_6)$	0 .28 .58 .88	0 .3 .7 1.1	0 .54 1.20 2.04	0 .9 2.1 3.7	0 1.4 3.2 5.9	0 .48 .91 1.50
$D' + \left\{ \begin{matrix} " \\ " \end{matrix} \right\} = "D+"$	3.27 3.81 4.81 6.18	10.7 12.6 15.8 19.3	7.1 8.0 10.4 13.9	5.9 7.7 11.4 18.2	6.8 9.4 15.3 26.3	2.75 3.45 4.80 6.86
$D' - \left\{ \begin{matrix} " \\ " \end{matrix} \right\} = "D-"$	3.25 3.65 4.42	12.0 14.4 17.1	7.0 8.0 9.8	5.9 7.2 10.8	6.6 8.9 14.5	2.59 2.98 3.86
$Sm^2/1000 = .26\ m^2 = s$	.26	.26	1.05	2.35	4.17	2.35
$\frac{b\tau}{a}m = .86\tau m$	0 .22 .43 .65	Same as for $\beta = .43$ (since $n' = 1$ when $n = 1$)				0 .65 1.29 1.93
n' (fig. 5a)	1 1 1 1					1 1 1.29 1.93
$\frac{b\tau}{an'} = .86\frac{\tau}{n'}$	0 .22 .43 .65					0 .22 .33 .33
λ (fig. 5b)	1 1.01 .80 .59					1 1.01 .92 .92
$\frac{s}{\lambda} D+ = "S+"$	.84 .97 1.55 2.70	2.79 3.22 5.06 8.50	7.5 8.3 13.5 24.7	18.0 33.5 72	88.5 39.2 80 184	6.37 7.88 12.1 17.3
$\frac{s}{\lambda} D- = "S-"$	.83 1.18 1.93	3.06 4.61 7.52	7.3 10.5 17.4	13.8 21.2 43	27.4 47 102	5.96 7.5 9.7
Negative Shear/1000 $S+/s_s$	∞ 10.6 8.6 9.8	∞ 8.8 6.9 7.6	∞ 5.8 4.82 5.6	∞ 5.5 5.1 7.3	∞ 6.9 6.9 10.7	∞ 9.5 7.3 6.9
Eq.Neg.Shear & Comp./1000 $S+/(s_s+s_c)$	4.6 3.6 4.3 6.0	3.8 2.9 3.5 4.8	2.6 2.0 2.4 3.5	2.2 1.87 2.6 4.5	2.5 2.3 3.6 6.7	3.8 3.2 3.7 4.3
Compression/1000 $S-/s_c$	4.6 4.5 6.4 10.4	3.8 4.1 6.2 10.2	2.6 2.5 3.6 5.9	2.2 2.12 3.2 6.5	2.5 2.4 4.0 8.7	3.8 3.6 4.5 5.8
Eq.Pos.Shear & Comp./1000 $S-/(s_s+s_c)$	4.6 3.0 3.3 4.2	3.8 2.8 3.2 4.2	2.6 1.7 1.9 2.5	2.2 1.44 1.6 2.7	2.5 1.7 1.7 3.7	3.8 2.4 2.3 2.4
Positive Shear/1000 $S-/s_s$	∞ 9.0 6.5 7.0	∞ 8.4 6.3 6.9	∞ 5.0 3.6 3.9	∞ 4.3 3.16 4.3	∞ 4.9 4.1 6.1	∞ 7.2 4.6 3.9

TABLE II

Stress combination	Positive shear	Equal positive shear and compression	Compression	Equal negative shear and compression	Negative shear
$S_{theor\ stab}$ (circles, fig. 11b)	3160	1440	2120	1870	4820
$S_{mat\ strength}$ (See par. 79)	3400	2000	2300	2000	3400
$\frac{S_{theor\ stab}}{S_{mat\ strength}}$	0.93	0.72	0.92	0.94	1/0.71
K_1 (fig. 6)	0.88	0.96	0.89	0.87	0.66
Critical m	3				2
Critical n	1				1
$\sqrt[4]{\frac{mn\ b}{10^5 t}} = \sqrt[4]{\frac{mn\ 12}{10^5 \times 0.19}}$	0.22				0.24
K_2 (fig. 7)	0.90				0.91
$F_{pract\ stab} = K_1 K_2 S_{theor\ stab}$	2500	1240	1700	1460	2880

TABLE III - Typical Tabular Solution of Case A' Problem

(Use similar form for Case B' problems except that B_1, B_2--, b_1, b_2--, B' are substituted for A_1, A_2--, a_1, a_2--, A')

$a(m = 1)$ n	24 2				24 1				36 1			
$\Delta_2 D_2 = D_2\left(\frac{1+830(n+1)/(n^2a^2D_2)}{1+830/(n\,a^2D_2)}\right)^2$	D_2 9.7 10.3				12.5 15.2				12.5 13.8			
$\beta = \frac{bm}{an} = \frac{14}{an}$	.29				.58				.39			
γ	0	.25	.50	.75	0	.25	.50	.75	0	.25	.50	.75
$A_1a_1 = 1.40\ a_1$ $A_2a_2 = .89\ a_2$ $A_3a_3 = 1.95\ a_3$	0 0 23.0	0 .1 23.5	0 .2 24.0	.1 .5 25.4	0 0 5.7	0 .1 6.1	.1 .2 6.8	.3 .6 8.1	0 0 12.5	0 .1 12.9	.1 .2 13.5	.1 .5 15.0
$\sum A_i a_i = A'$	23.0	23.6	24.2	26.0	5.7	6.2	7.1	9.0	12.5	13.0	13.8	15.6
$O_1o_1 = 1.36\ o_1$ $O_2o_2 = 3.84\ o_2$ $O_3o_3 = 2.15\ o_3$	.1 0 25.5	.1 0 25.8	.1 .1 26.2	.1 .2 28.0	.5 0 6.3	.5 .1 6.8	.5 .3 7.5	.5 .7 9.0	.2 0 14.0	.2 0 14.4	.2 .2 15.0	.2 .3 16.7
$\sum O_i o_i = O'$	25.6	25.9	26.4	28.3	6.8	7.4	8.3	10.2	14.2	14.6	15.4	17.2
$\left(\frac{\alpha}{mn}\right)^2 = \left(\frac{.395a}{n}\right)^2 = d_o$	22.4				90				202			
$"D_o"d_o = A'/O'\,d_o$ $D_1d_1 = .273\ d_1$ $(\Delta_2D_2)\ d_2$ $D_3d_3 = .273\ d_3$ $D_4d_4 = 1.38\ d_4$	20.2 0 121 .1 1.4	20.4 0 124 .3 1.4	20.6 0 127 .6 1.5	20.6 0 135 1.1 1.5	75 .1 44 .1 1.4	75 .1 48 .3 1.4	77 .1 53 .6 1.5	79 .1 64 1.1 1.7	178 .1 91 .1 1.4	180 .1 95 .3 1.4	181 .1 99 .6 1.5	183 .1 109 1.1 1.5
$\sum D_i d_i = D'$	143	146	150	158	121	125	132	146	271	277	282	295
$(D_5d_5 + D_6d_6) = -.178(d_5 + d_6)$	0	-.3	-.6	-.8	0	-.3	-.6	-.9	0	-.3	-.6	-.9
$D' + \left\{ \begin{matrix} " \\ " \end{matrix} \right\} = D+$ $D' - \left\{ \begin{matrix} " \\ " \end{matrix} \right\} = D-$	143 143	146 146	149 151	157 159	121 121	125 125	131 133	145 147	271 271	277 277	281 283	294 296
$Sm^2/1000 = 50/a^2 = z$	.086				.086				.039			
$z\ D+ = S+$ $z\ D- = S-$	12.3 12.3	12.6 12.6	12.8 13.0	13.5 13.7	10.4 10.4	10.7 10.7	11.3 11.5	12.5 12.7	10.6 10.6	10.8 10.8	11.0 11.1	11.5 11.6
s_s	0	.04	.08	.12	0	.17	.33	.51	0	.08	.15	.22
$\left(1 + \frac{E_b'A_b'}{E_b t\,a^2}\right)s_b = 1.87\ s_b$ $1.87\ s_b + s_s$	1.87 1.87	1.89 1.93	1.92 2.00	2.00 2.12	1.87 1.87	1.94 2.11	2.05 2.38	2.24 2.75	1.87 1.87	1.93 2.01	2.00 2.15	2.05 2.27
Eq.Pos.Shear & Compression/1000 $S+/(1.87s_b+s_s)$ Compression/1000 $S+/(1.87s_b)$	6.6 6.6	6.5 6.7	6.4 6.7	6.4 6.8	5.6 5.6	5.1 5.5	4.7 5.5	4.5 5.6	5.7 5.7	5.4 5.6	5.1 5.5	5.1 5.6
Eq.Neg.Shear & Compression/1000 $S-/(1.87s_b+s_s)$	6.6	6.6	6.5	6.5	5.6	5.1	4.8	4.6	5.7	5.4	5.2	5.1

TABLE IV

	Stress combination	Positive shear	Equal positive shear and compression	Compression	Equal negative shear and compression	Negative shear
Sheet	$S_{theor\ stab}$ (circles, fig. 12)		4500	5500	4600	
	$S_{mat\ strength}$		2000	2300	2000	
	$\frac{S_{mat\ strength}}{S_{theor\ stab}}$		0.44	0.42	0.43	
	K_1 (fig. 6)		0.43	0.40	0.41	
Stiffener	$S_{theor\ stab}$ (compression only) $S_b' = \frac{1.05 \times 1700000}{342000} S_b = 5.2 S_b$		23500	28600	24000	
	$S_{mat\ strength}$ (reference 1, p. 14)		7000	7000	7000	
	$\frac{S_{mat\ strength}}{S_{theor\ stab}}$		0.30	0.25	0.29	
	K_1 (fig. 6)		0.29	0.24	0.28	
	Critical a, n			24,1		
	$\sqrt[4]{\frac{mn\ a}{10^5 t'}} = \sqrt[4]{\frac{1 \times 1 \times 24}{10^5 \times 0.44}}$			0.15		
	K_2 (fig. 7)			0.94		
Sheet	$F_{pract\ stab} = K_1 K_2 S_{theor\ stab}$		1220	1240	1220	
	$F_{pract\ stab}$ (from table II)	2500	1240	1700	1460	2880
	$F_{pract\ stab}$ (critical)	2500	1220	1240	1220	2880

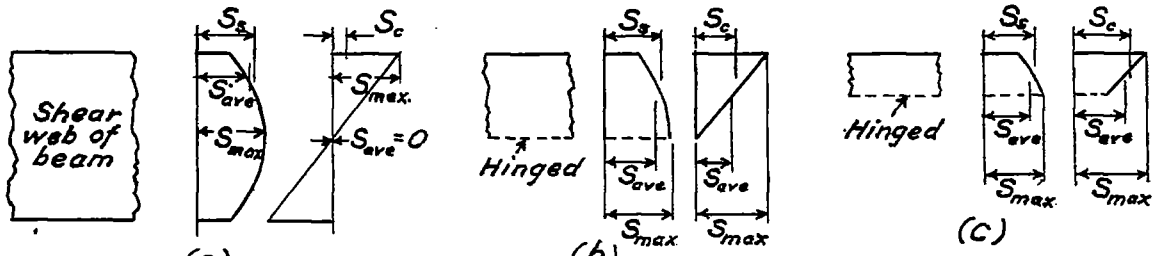

Figure 1

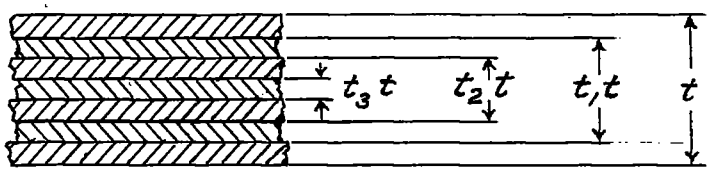

Figure 2

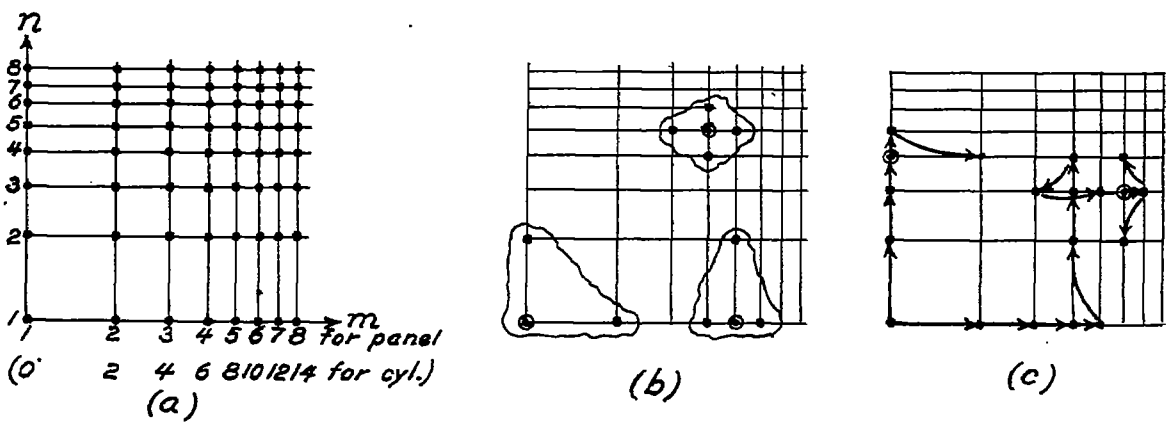

Figure 4

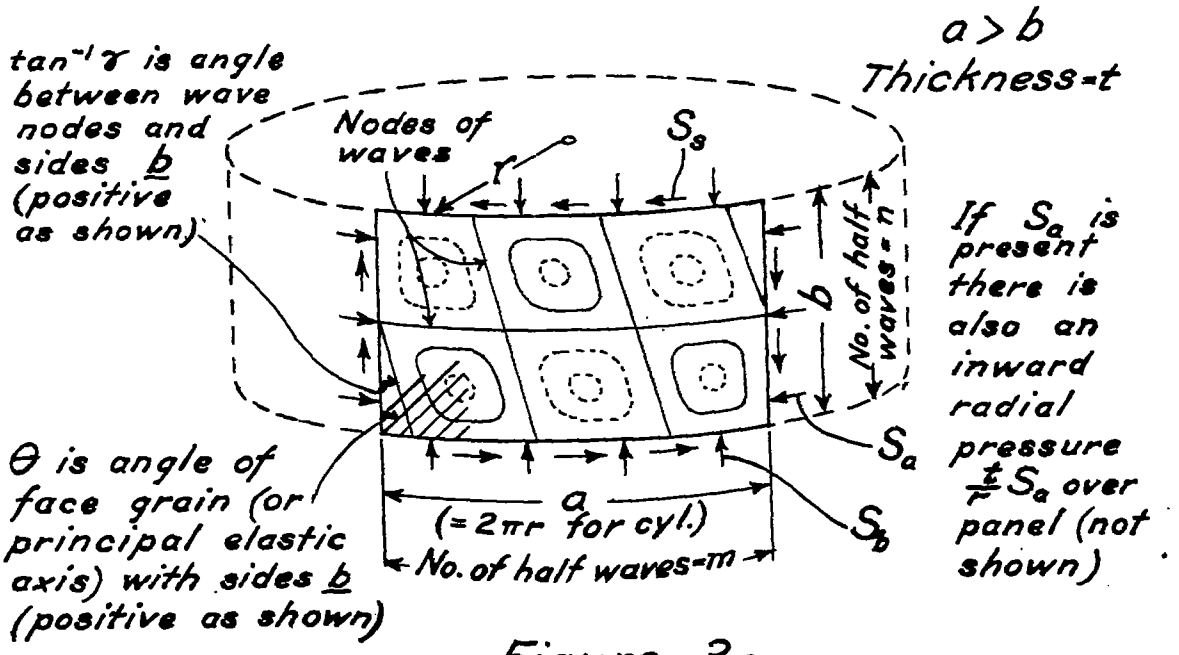

Figure 3a

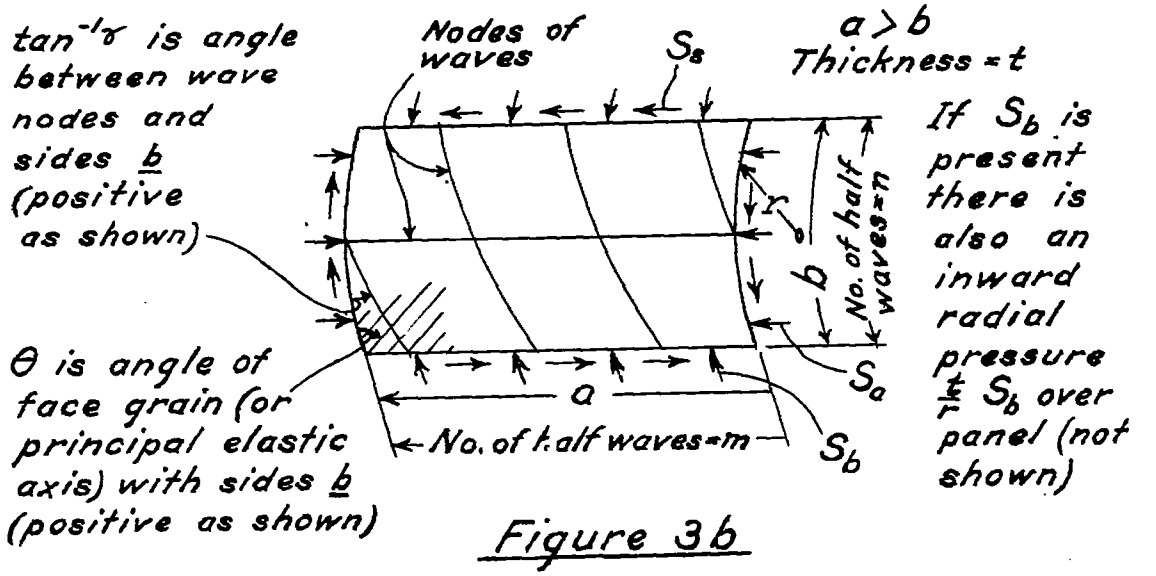

Figure 3b

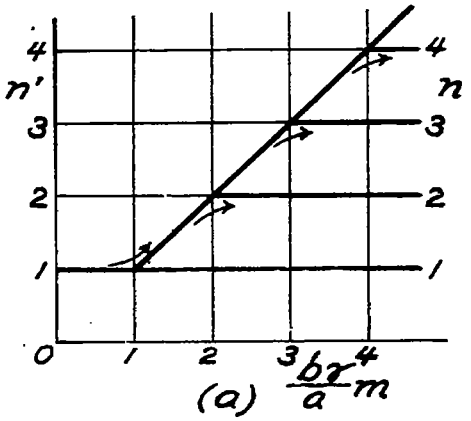

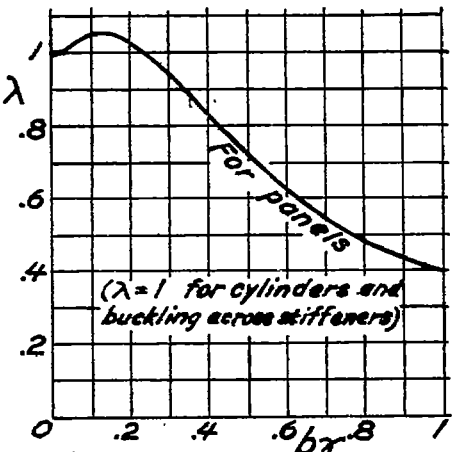

Figure 5

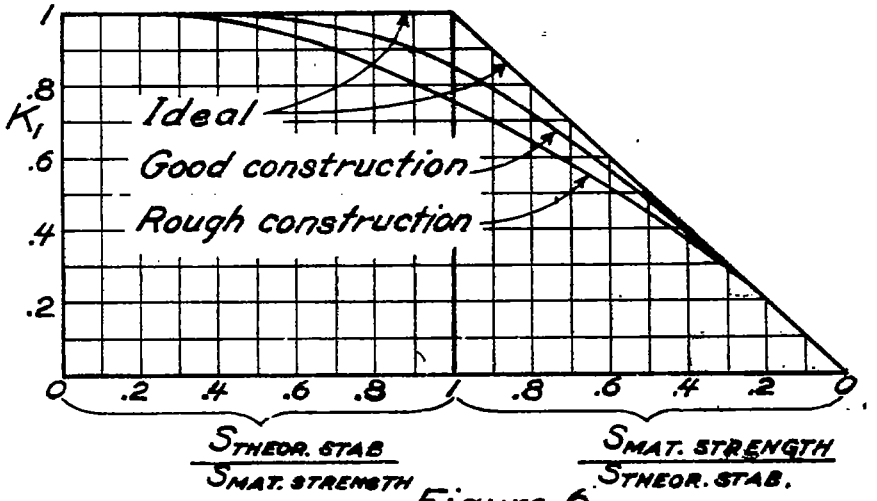

Figure 6

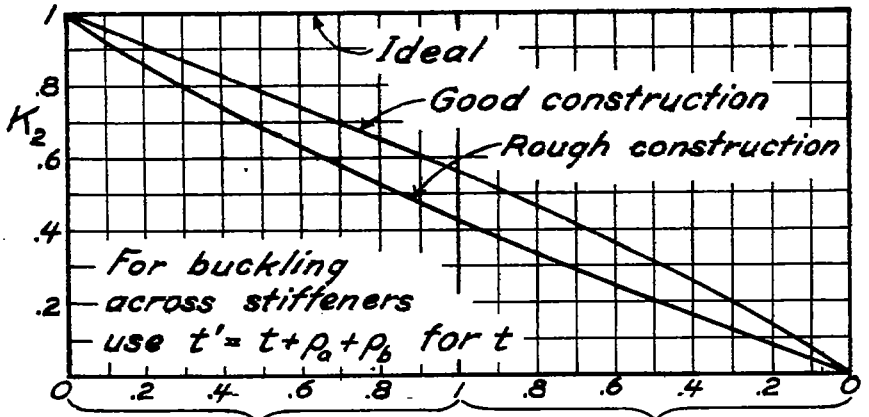

Figure 7

(*Change a to b for Case B)

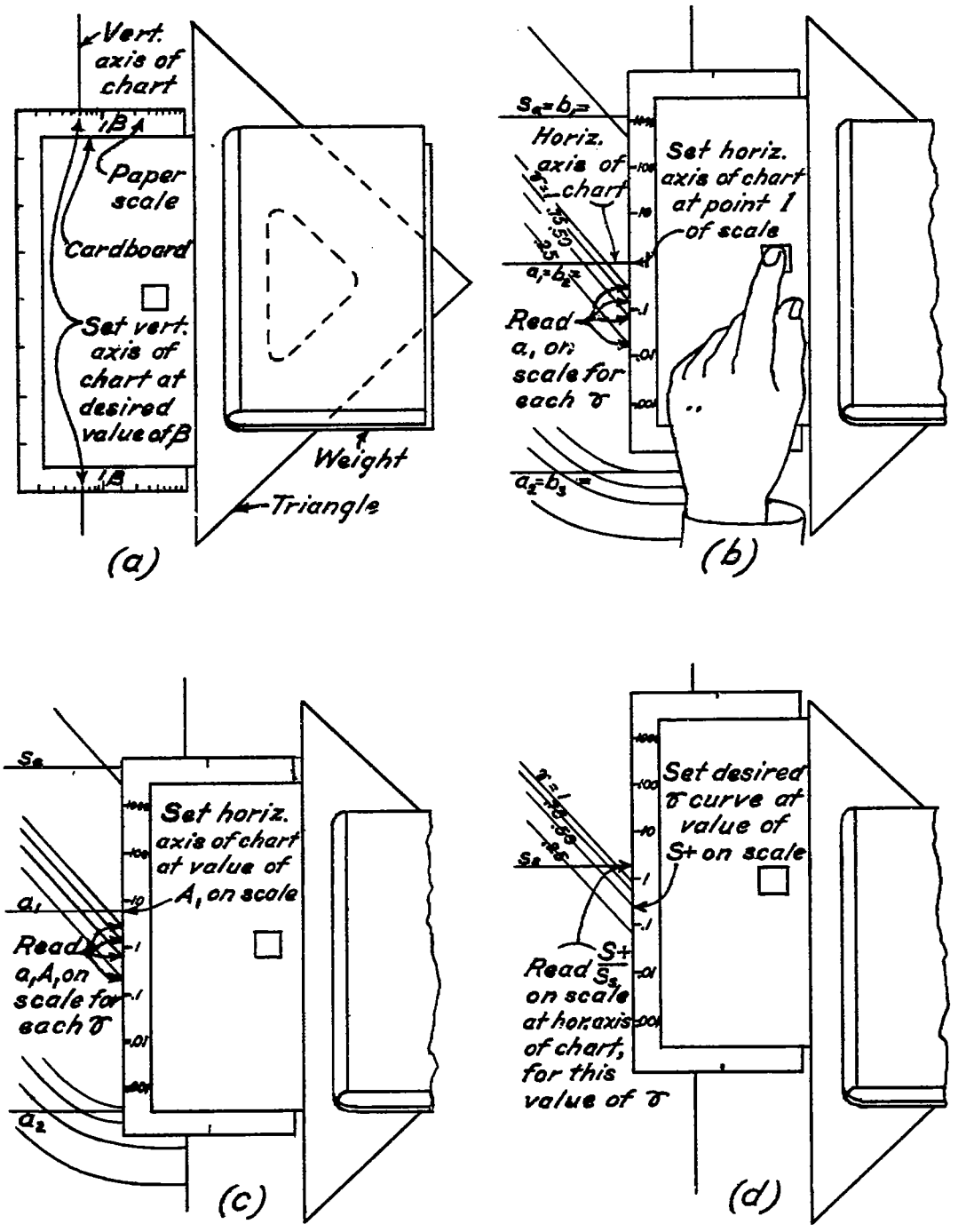

Figure 8

Method of using figure 9.

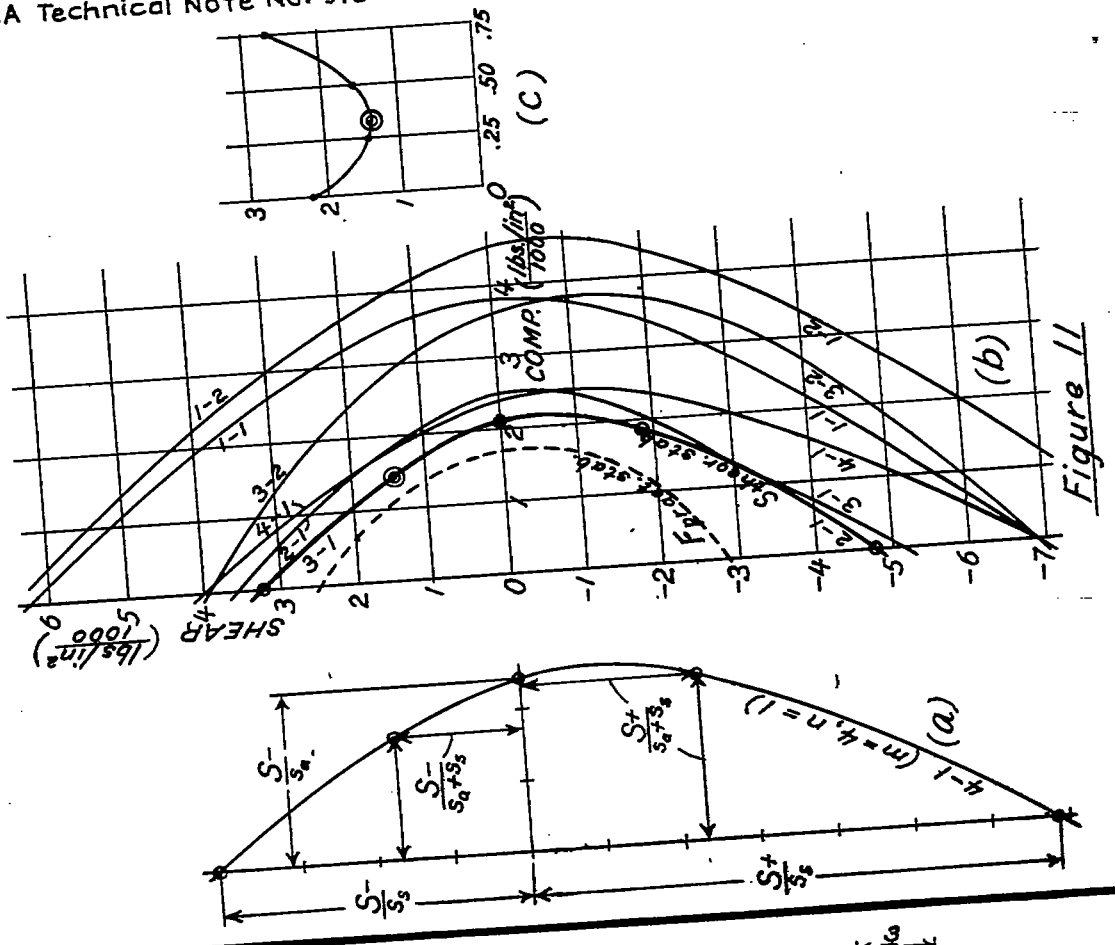

Figure 11

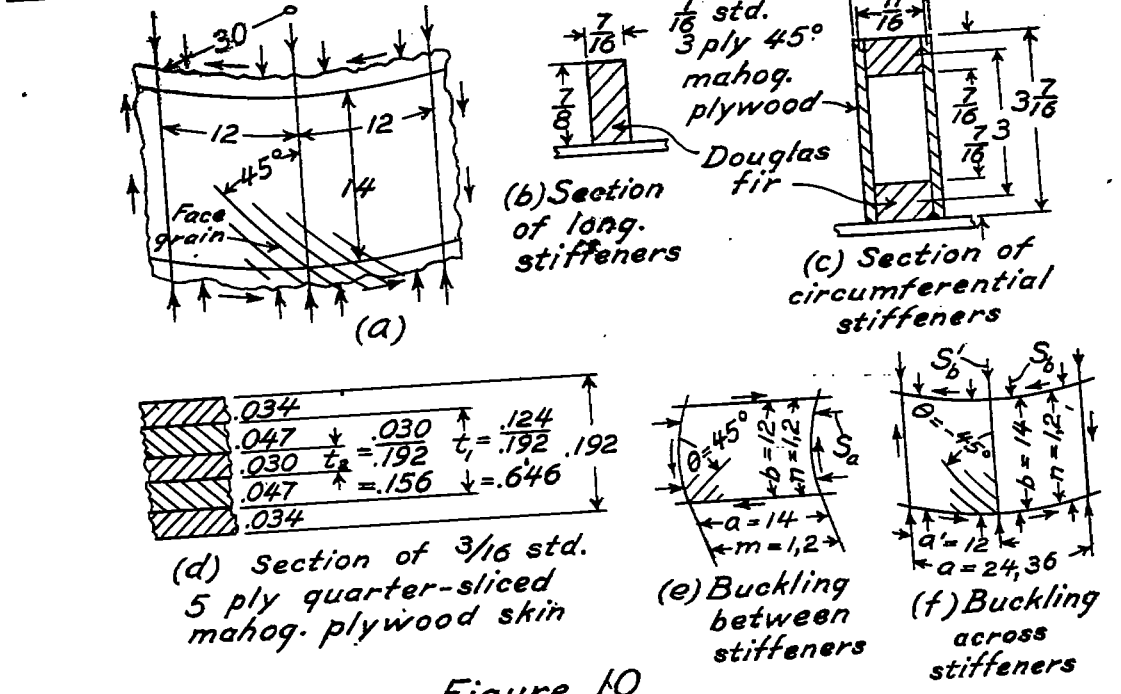

Figure 10

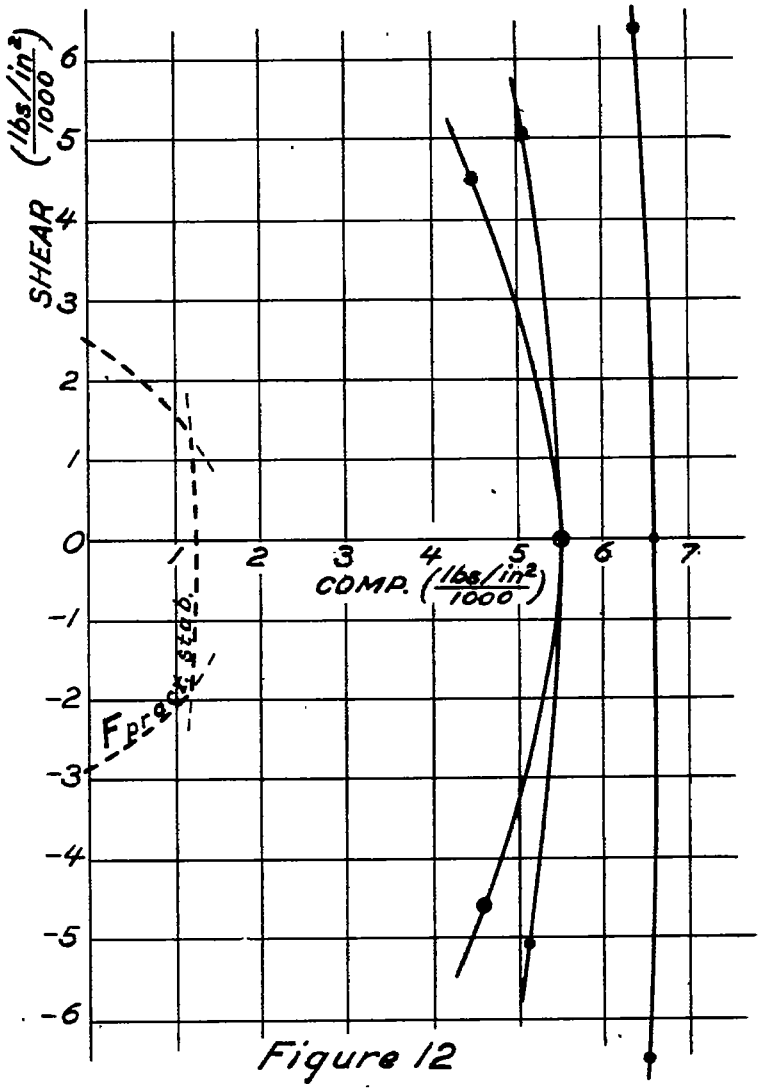

Figure 12

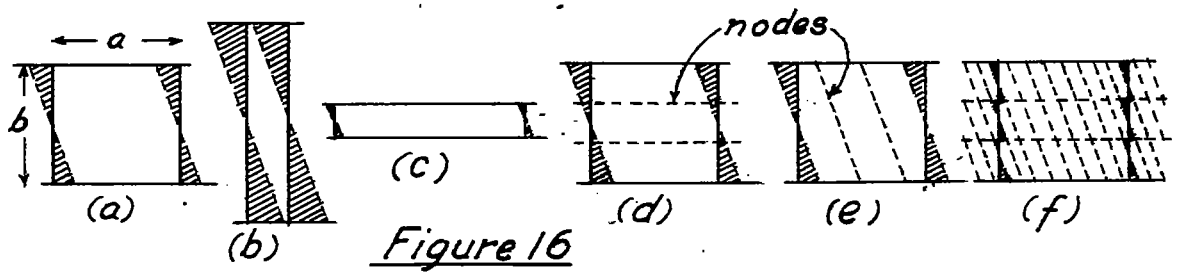

Figure 16

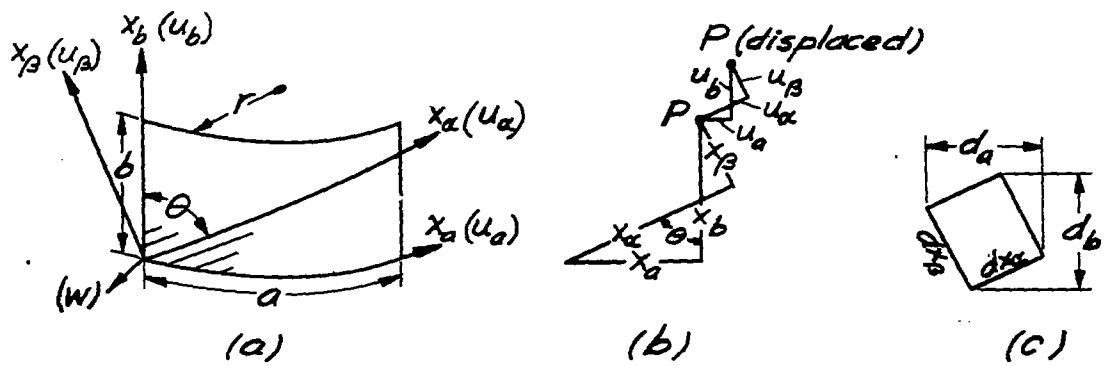

Figure 13

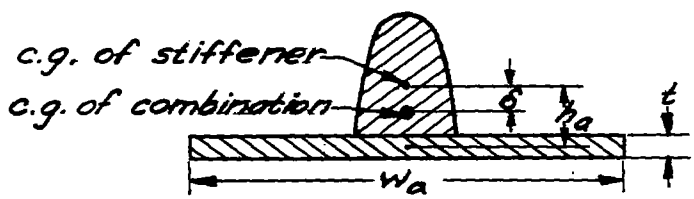

Figure 14

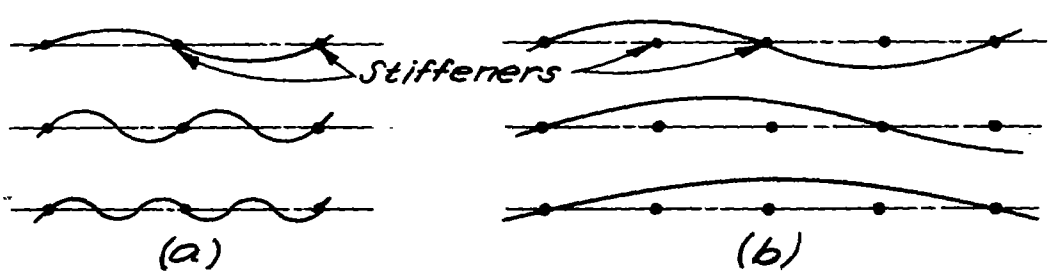

Figure 15

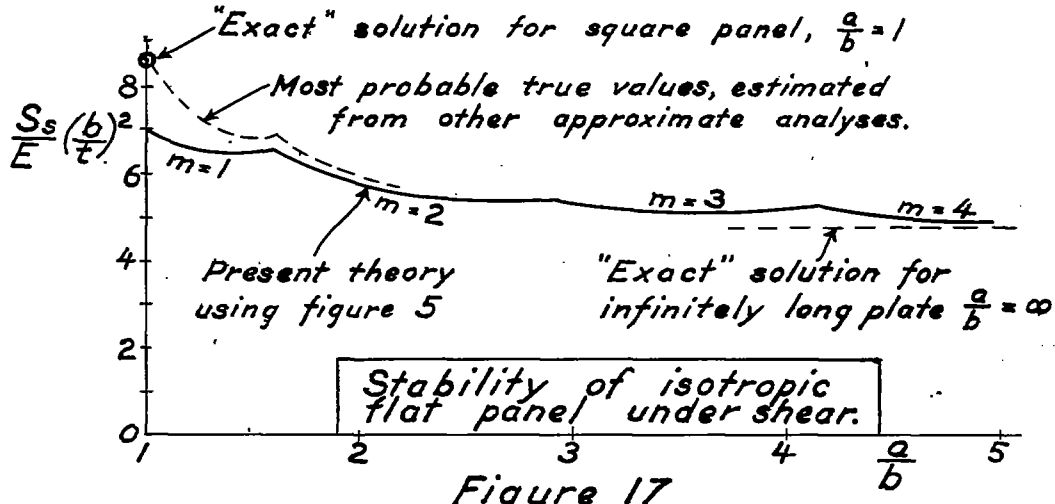

Figure 17

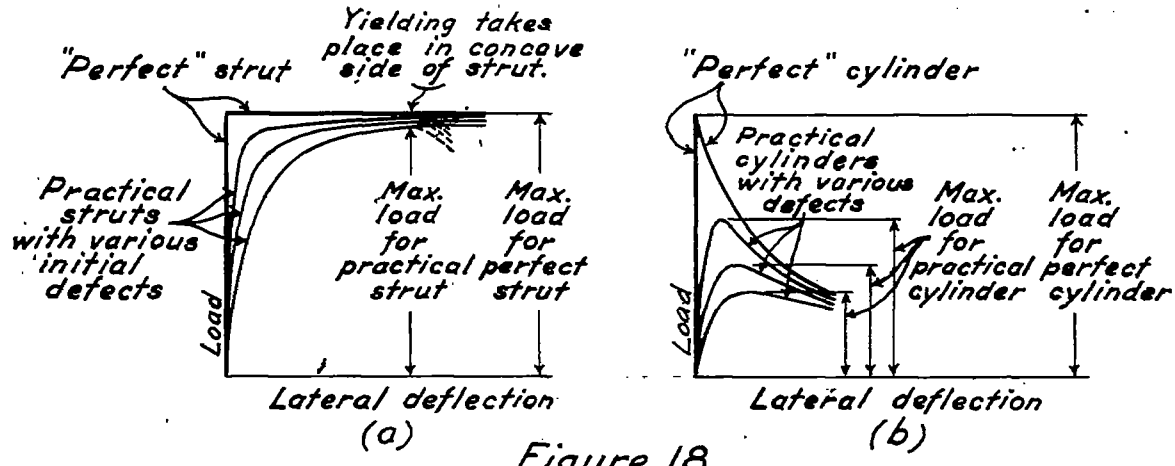

Figure 18

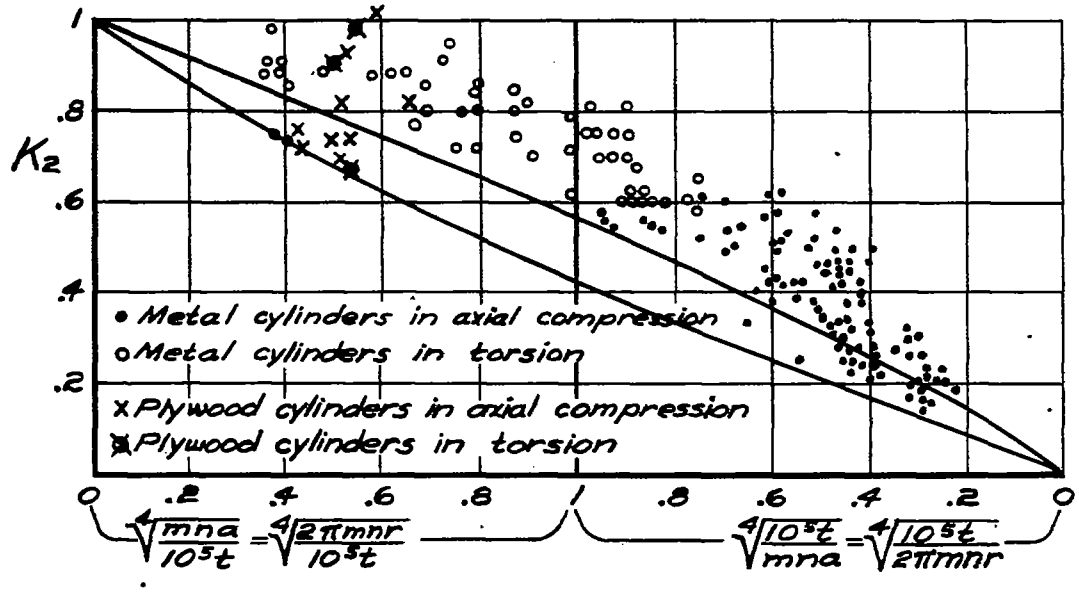

Figure 19

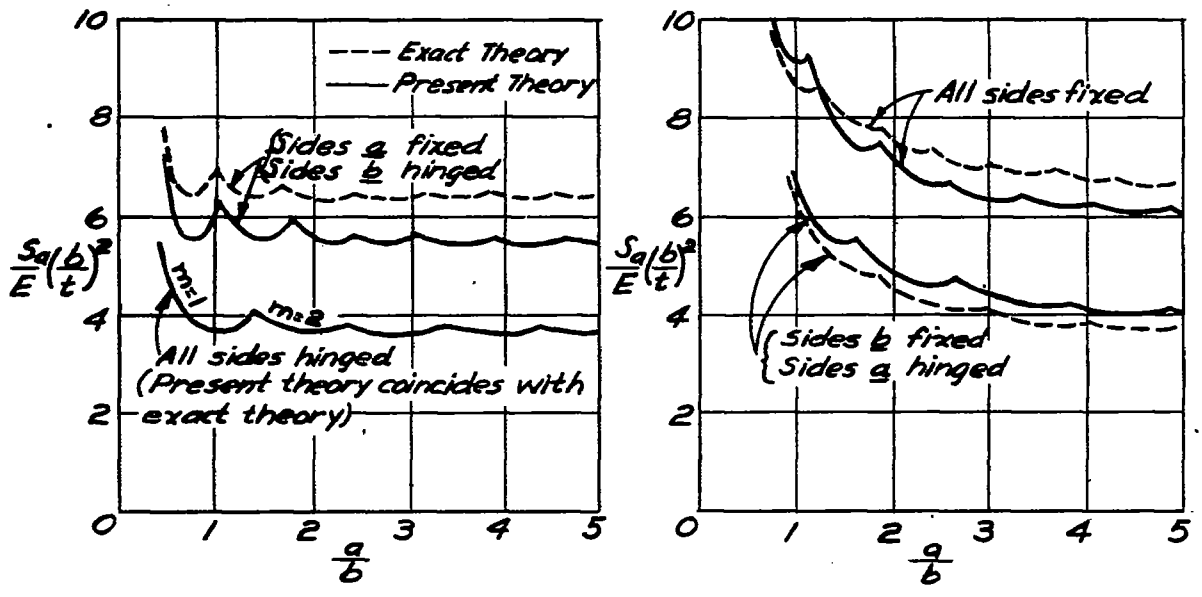

Figure 20

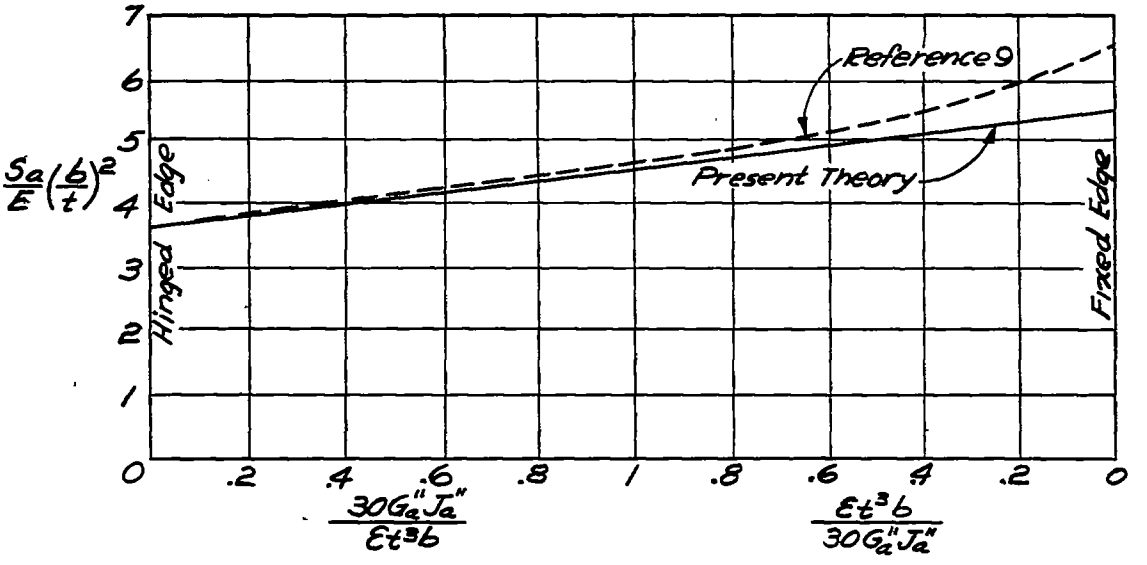

Figure 21

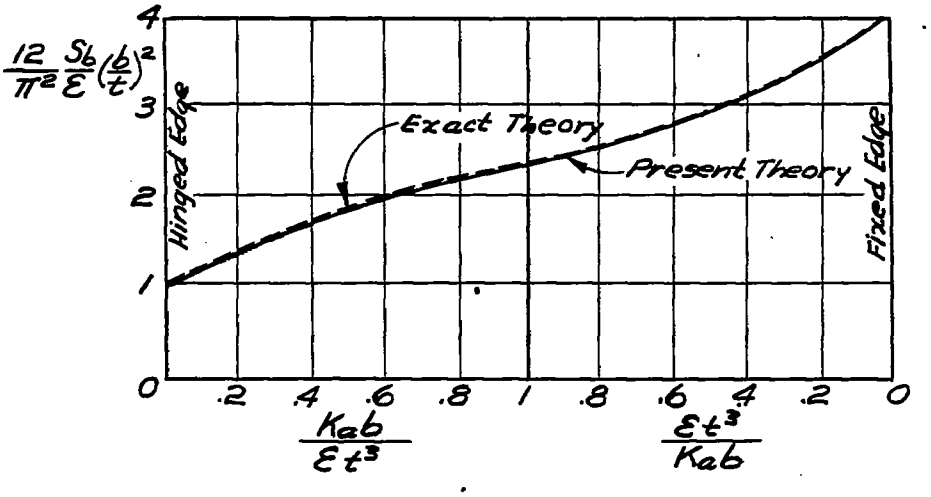

Figure 22

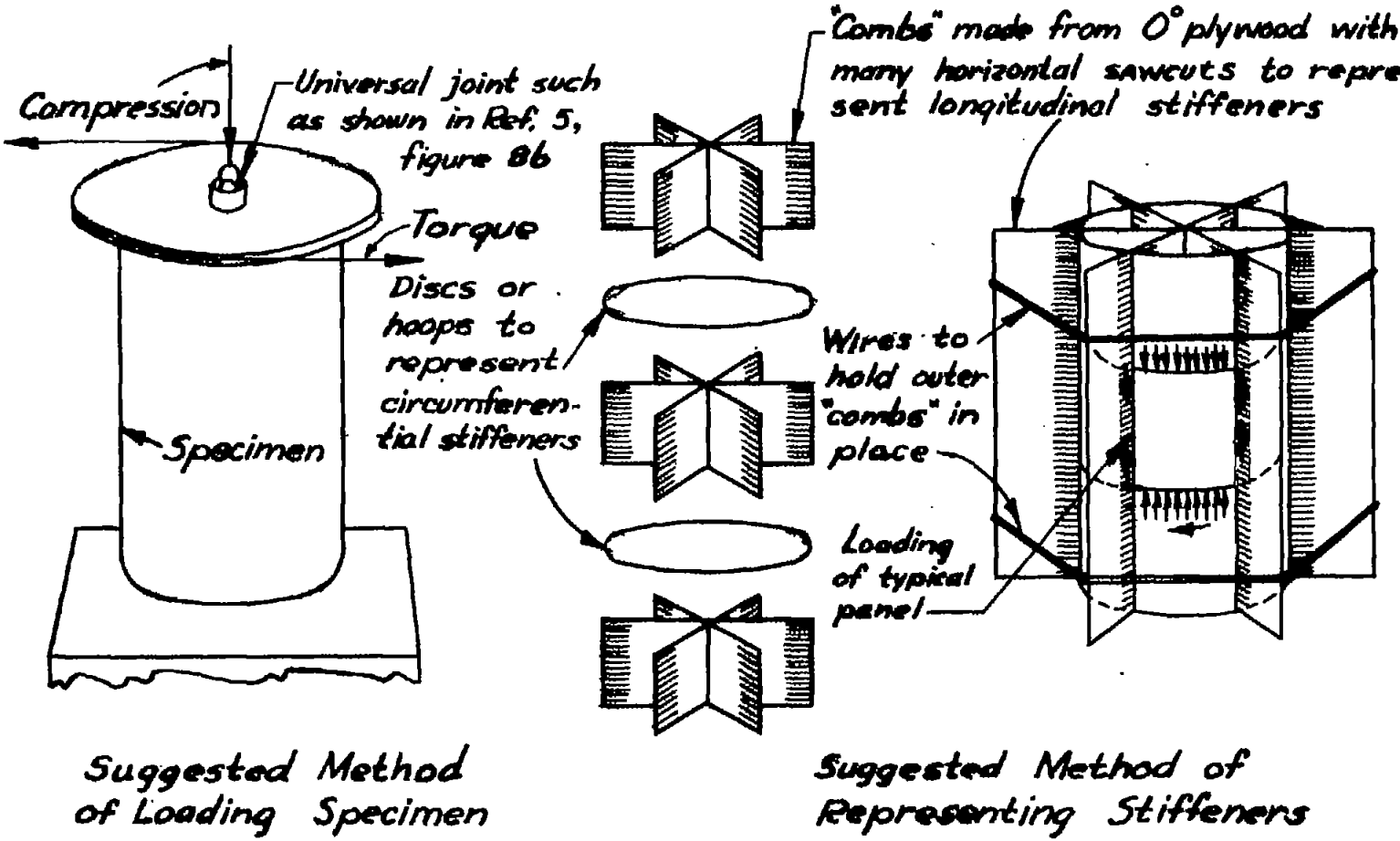
Compression
Universal joint such as shown in Ref. 5, figure 86
Torque
Specimen
Discs or hoops to represent circumferential stiffeners
"Combs" made from 0° plywood with many horizontal sawcuts to represent longitudinal stiffeners
Wires to hold outer "combs" in place
Loading of typical panel
Suggested Method of Loading Specimen
Suggested Method of Representing Stiffeners

Figure 23

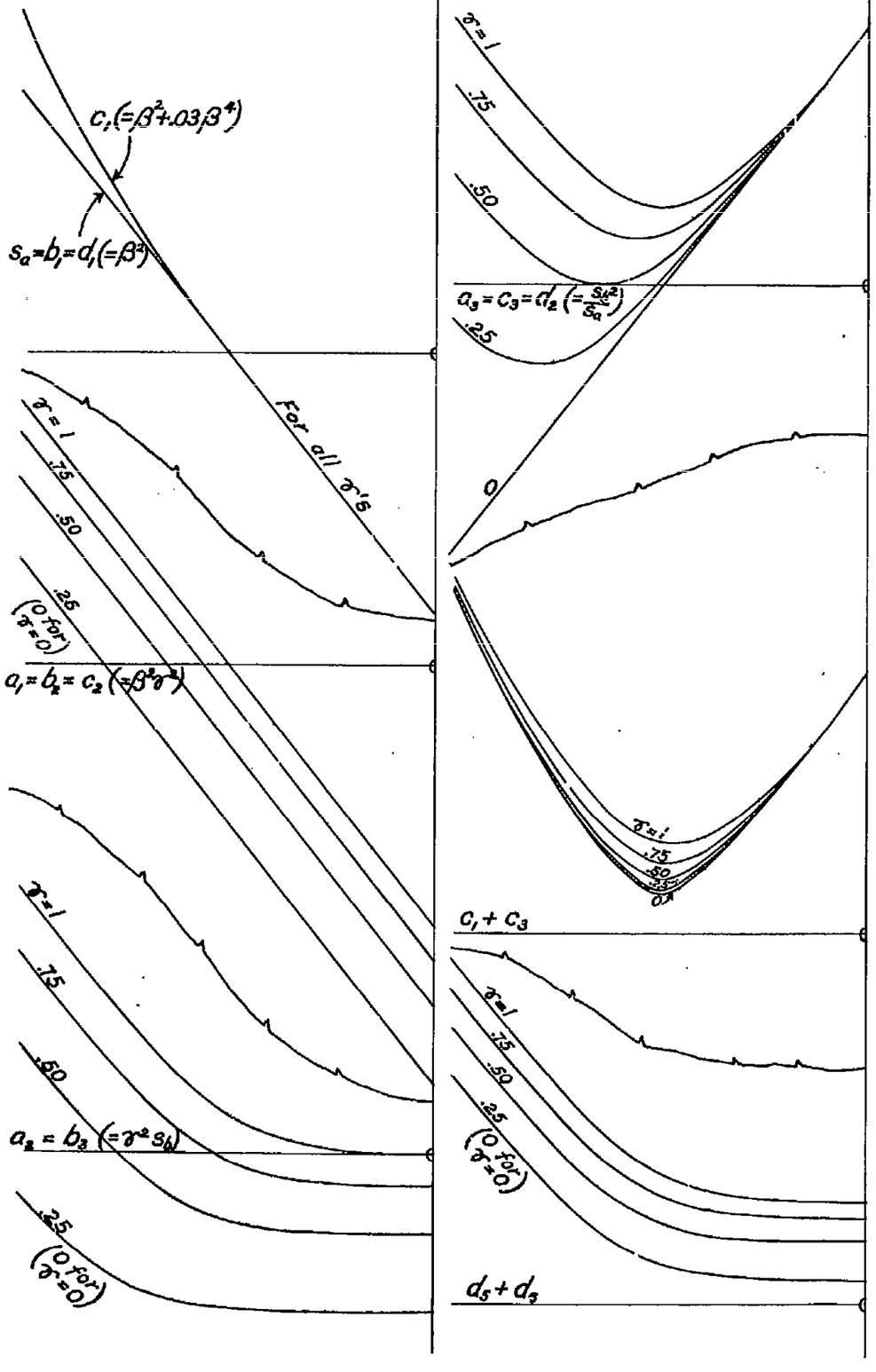

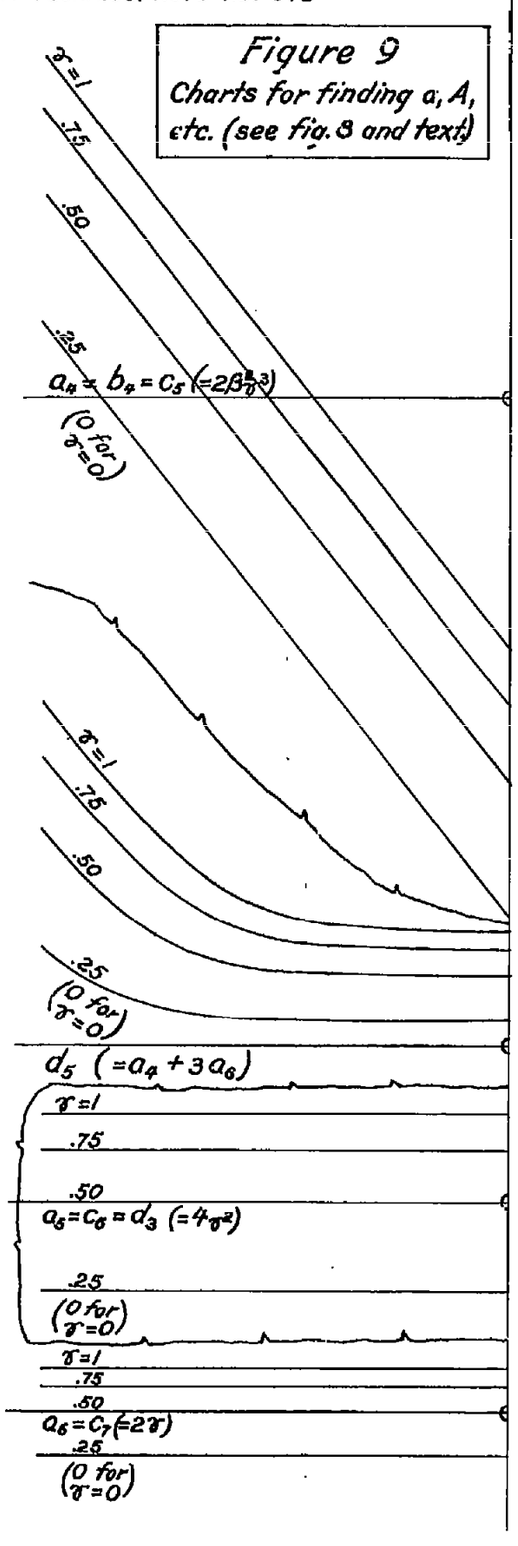

Figure 9
Charts for finding a, A, etc. (see fig. 8 and text)

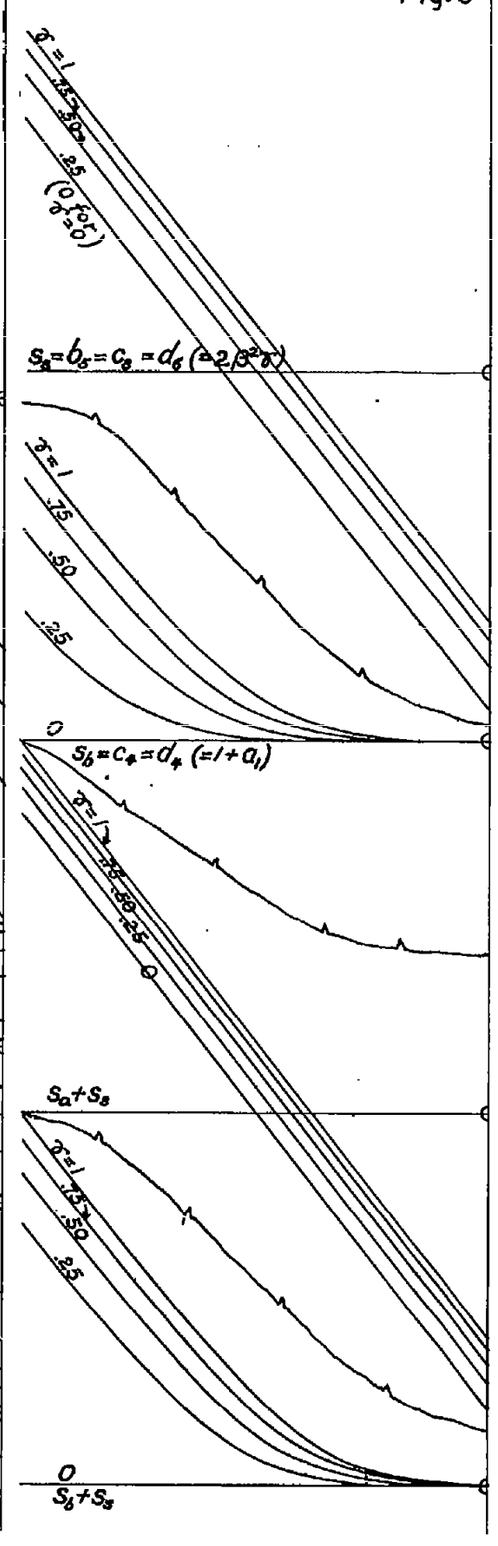

Cement heavy cardboard, such as used for backing of pads, to paper scale, as shown by dotted lines. A small hole may be cut in cardboard as shown before cementing, to give better grip in sliding.

If water paste or glue must be used, cement corners only, to avoid distorting paper scale. This edge of cardboard must be <u>straight</u> and <u>parallel</u> to PP. Use scale as shown in Figure 8.